

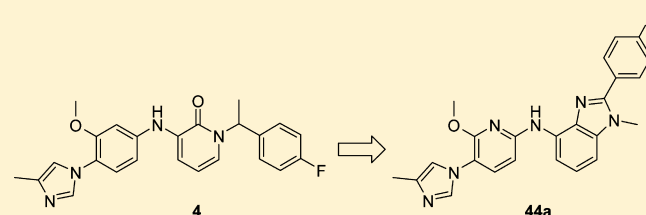
## Design and Synthesis of a Novel Series of Bicyclic Heterocycles As Potent $\gamma$ -Secretase Modulators

Francois Bischoff, Didier Berthelot, Michel De Cleyn, Gregor Macdonald, Garrett Minne, Daniel Oehlich, Serge Pieters, Michel Surkyn, Andrés A. Trabanco, Gary Tresadern, Sven Van Brandt, Ingrid Velter, Mirko Zaja, Herman Borghys, Chantal Masungi, Marc Mercken, and Harrie J. M. Gijssen\*

Janssen Research & Development, Pharmaceutical Companies of Johnson & Johnson, Beerse, Belgium

### S Supporting Information

**ABSTRACT:** The design and the synthesis of several chemical subclasses of imidazole containing  $\gamma$ -secretase modulators (GSMs) is described. Conformational restriction of pyridone **4** into bicyclic pyridone isosteres has led to compounds with high in vitro and in vivo potency. This has resulted in the identification of benzimidazole **44a** as a GSM with low nanomolar potency in vitro. In mouse, rat, and dog, this compound displayed the typical  $\gamma$ -secretase modulatory profile by lowering  $A\beta_{42}$  and  $A\beta_{40}$  levels combined with an



especially pronounced increase in  $A\beta_{38}$  and  $A\beta_{37}$  levels while

### INTRODUCTION

Alzheimer's disease (AD) is a chronic and progressive neurodegenerative disorder characterized by the deposition of extraneuronal amyloid plaques and intraneuronal neurofibrillary tangles of hyperphosphorylated tau protein in the limbic and cortical regions of the brain.<sup>1</sup> These pathological depositions were first discovered in 1906 by Alois Alzheimer during the autopsy of patients with loss of memory, cognition, and behavioral stability.<sup>2</sup> Nowadays, AD is the leading form of dementia and the third leading cause of death after cardiovascular disease and cancer.

AD does not have a simple etiology, but a substantial body of evidence supports the amyloid hypothesis which supposes that the accumulation of the amyloid- $\beta$  peptide ( $A\beta$ ) caused by altered production or clearance is the causative event in AD.<sup>3</sup>  $A\beta$ -peptides are derived from the amyloid precursor protein (APP) by two sequential proteolytic cleavages. The first cleavage of APP is catalyzed by the aspartyl protease BACE1 ( $\beta$ -secretase), yielding a soluble N-terminal fragment (sAPP) which is excreted from the cell, and a short membrane-bound C-terminal fragment (C99). The latter is a substrate for  $\gamma$ -secretase, and it is cleaved at variable positions of the transmembrane domain to release a 37–43 amino acid long  $A\beta$ -peptide. The two most common forms of  $A\beta$  produced in this way are  $A\beta_{40}$  and  $A\beta_{42}$ , containing 40 and 42 amino acid residues respectively. It is the longer and more hydrophobic  $A\beta_{42}$  that forms the nucleus of the amyloid plaques and is thought to cause the neurotoxicity associated with AD.

The search for  $\gamma$ -secretase inhibitors (GSIs) that lower the production of all  $A\beta$  isoforms has been a first strategy to prevent the formation of amyloid plaques. Several GSIs have moved to the clinic, and their progress has been reviewed recently.<sup>4</sup> The development of the most advanced compound,

semagacestat, was interrupted during a phase III clinical trial as it was associated with worsening of clinical measures of cognition and an increase in the risk of skin cancer. Multiple reasons have been proposed to explain the lack of efficacy and observed side effects, including the rebound effect on  $A\beta_{42}$  at low levels of semagacestat, poor selectivity versus Notch cleavage, and accumulation of neurotoxic C99.<sup>4b,5</sup> In contrast to GSIs,  $\gamma$ -secretase modulators (GSMs) are defined as molecules that change the relative proportion of the  $A\beta$  isoforms while maintaining the rate at which APP is processed.<sup>6</sup> Targeted modulation of  $\gamma$ -secretase activity in such a way that the release of the longer amyloidogenic  $A\beta$ -peptides, especially  $A\beta_{42}$ , is disfavored with regard to the shorter and more soluble  $A\beta$ -peptides, especially  $A\beta_{37}$  and  $A\beta_{38}$ , has been and still is an important strategy to tackle AD.<sup>7,8</sup> Mechanistically, GSMs have been postulated to act as activators of the  $\gamma$ -secretase complex, enhancing the stepwise cleavage of APP toward the shorter  $A\beta$ -peptides.<sup>9</sup> In a recent study to further discriminate between modulation and inhibition, a GSM successfully improved cognitive deficits in APP-transgenic mice whereas a GSI caused cognitive impairment likely due to accumulation of C99.<sup>5</sup>

Two major classes of compounds are known to modulate the  $\gamma$ -secretase activity.<sup>10</sup> The first of these are carboxylic acids derived from nonsteroidal anti-inflammatory drugs (NSAIDs).<sup>11</sup> Initial examples of this class, such as tarenfluril (**1**), were of low potency and displayed poor brain penetration, resulting in the failure of **1** in phase III clinical trials (Figure 1). Subsequent, more potent analogues suffered from very high

**Special Issue:** Alzheimer's Disease

**Received:** December 20, 2011

**Published:** May 31, 2012

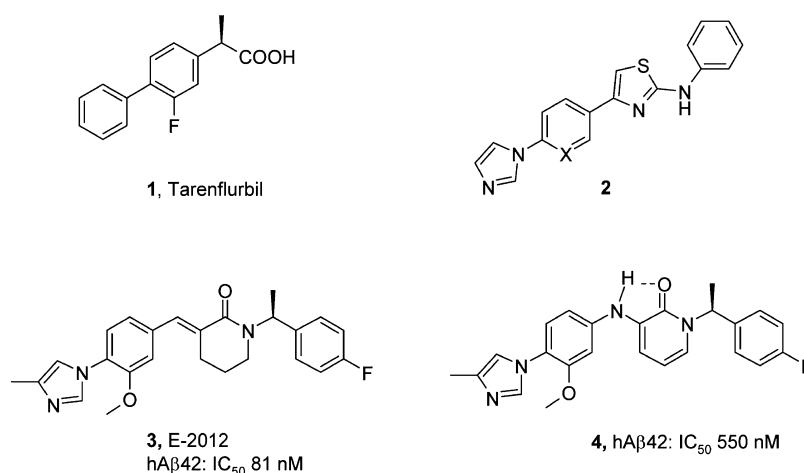
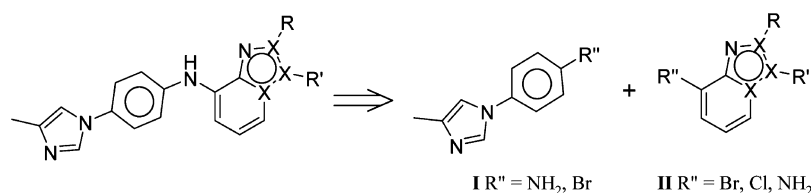


**Figure 1.** Examples of  $\gamma$ -secretase modulators. In vitro data were obtained from in-house experiments. The IC<sub>50</sub> values are a mean of at least three determinations.

### Scheme 1



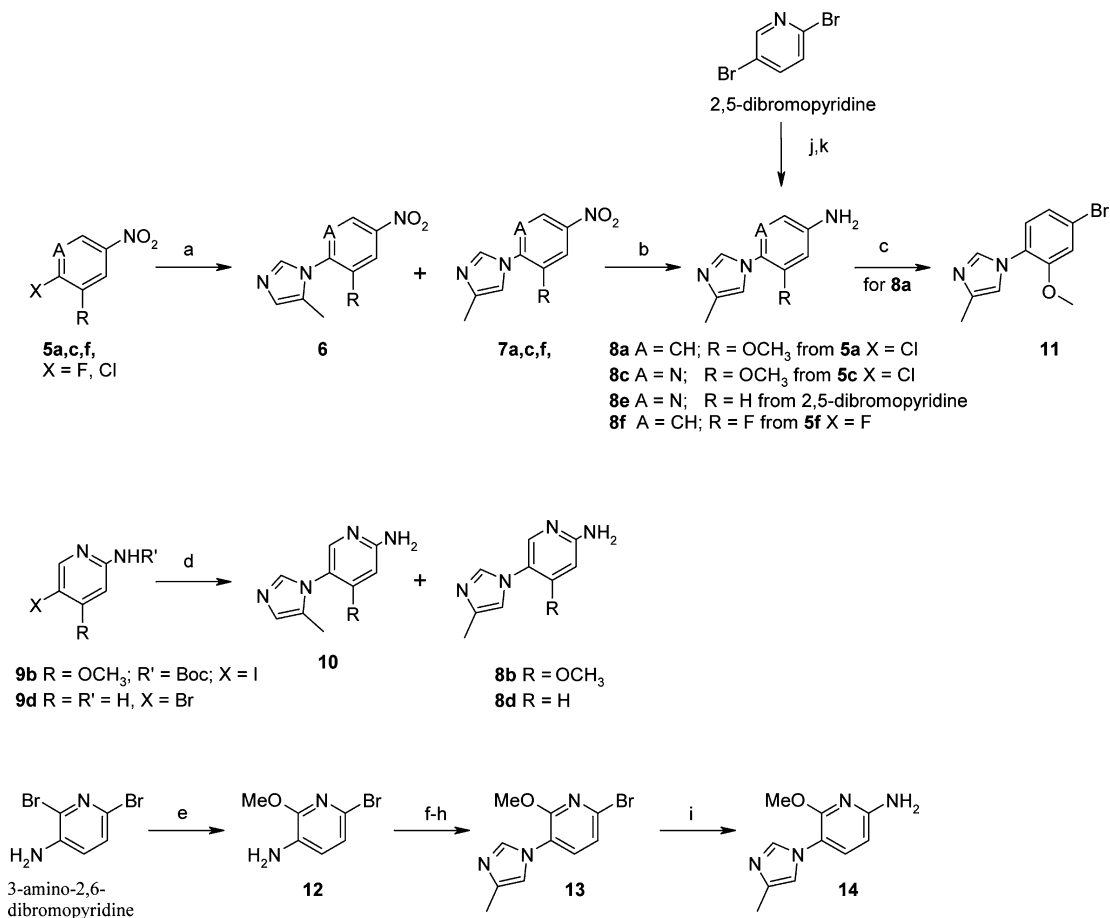
lipophilicity, limiting the potential use of these compounds as GSMs. The second class of GSMs is characterized by non-NSAID-scaffolds without a carboxylic acid group. These were initially reported by Neurogenetics in 2004, claiming imidazole containing compounds of general structure **2** as  $A\beta$ -modulating agents with potencies below 1  $\mu$ M.<sup>12</sup> Subsequent work by Eisai has led to E-2012 (**3**), the first compound from this series entering the clinic (Figure 1).<sup>13</sup> However, further development of E-2012 was halted due to lenticular toxicity in preclinical trials.<sup>6</sup> Compound **3** was used as a starting point for the design of our own non-NSAID  $\gamma$ -secretase modulators for the treatment of AD.<sup>14</sup>

The cinnamide group in **3** has an *E* orientation of the double bond. Our first hit was obtained by speculating that an NH linker as in compound **4** would preserve a similar geometry due to favorable electrostatic interaction between the NH and the carbonyl oxygen. Also, a steric clash between the carbonyl and the methoxyphenyl ring of **4** would disfavor alternative conformations. Computational modeling of **4** suggested that the orientation as sketched was the most energetically favorable conformation.<sup>15</sup> This type of aminopyridones has also been described by Schering/Merck, including **4**.<sup>14a</sup> Despite the conformational similarity between **3** and **4**, subsequent testing of both compounds in vitro showed a loss in potency of **4** versus **3** (550 vs 81 nM, respectively). Upon oral administration in mice at 30 mg/kg, no significant change in  $A\beta$  brain levels was observed after 4 h for **4**, while dosing of **3** resulted in a 43% reduction of  $A\beta$ 42 levels. To improve the in vitro potency and in vivo activity of **4**, we set out to further conformationally restrict the aminopyridone scaffold in **4**. In this paper, we will discuss our findings in this area and the development of a number of subseries with high in vitro and in vivo potency.<sup>16</sup>

### CHEMISTRY

All the final compounds were synthesized via a Buchwald coupling between the anilino- or bromo-derivatives **I** and the corresponding halo- or anilino- heterocyclic intermediates **II**, respectively (Scheme 1).

**Synthesis of Intermediates I.** In a first approach, the aniline precursors (**I**, R'' = NH<sub>2</sub>) were prepared in two steps, starting from commercially available 4-halo-nitroarenes, as exemplified for anilines **8(a,c,f)** in Scheme 2. Nucleophilic aromatic substitution of a 4-halide in **5** with 4-methylimidazole gave a mixture of regioisomers, from which **7** was isolated in good yield. Subsequent catalytic hydrogenation of the nitro functionality in **7** provided the desired anilines **8(a,c,f)** in good yields. **8a** could then be submitted to Sandmeyer reaction conditions to provide the bromo precursor **11** (I, R'' = Br). In another approach, the selective substitution of the 5-bromide in 2,5-dibromopyridine with 4-methylimidazole followed by a copper oxide amination with ammonium hydroxide afforded aniline **8e**.<sup>17</sup> Alternatively, compounds **8b** and **8d** were prepared in one step, via an Ullmann type coupling of the 4-methylimidazole with 4-halo-anilines **9b** and **9d**, respectively.<sup>18</sup> Separation of the two regioisomers provided the major, and desired, regioisomers **8b** and **8d** in good yields. A different approach was used for synthesis of the pyridylmethoxy derivative **14**. Regioselective nucleophilic addition of sodium methoxide to commercially available 3-amino-2,6-dibromopyridine provided the methoxypyridylamine **12**.<sup>19</sup> The amine moiety in **12** was converted to the desired 4-methylimidazole ring in **13** in a sequence of reactions that included formylation with acetic formic anhydride,<sup>20</sup> followed by alkylation with 1-chloropropanone and finally ring closure of the resulting formyloxopropyl amine with ammonium acetate. Bromo-intermediate **13** could easily be converted to amino-derivative

Scheme 2. General Synthetic Route Towards Intermediates I<sup>a</sup>

<sup>a</sup>Reagents and conditions: (a) 4-methylimidazole, K<sub>2</sub>CO<sub>3</sub>, DMSO, 150 °C, 6 h; (b) H<sub>2</sub>, Pd(C), MeOH, 50 °C, 12 h; (c) NaNO<sub>2</sub>, H<sub>2</sub>SO<sub>4</sub>, 10 °C, 30 min, then CuBr, HBr; 10 °C to rt, 1 h; (d) 4-methylimidazole, CuI, 1,10-phenanthroline, Cs<sub>2</sub>CO<sub>3</sub>, DMSO, 130 °C, 2 d; (e) NaOMe, 1,4-dioxane, rt, 8 h; (f) AcOH, HCO<sub>2</sub>H, THF, 60 °C, 12 h; (g) 1-chloropropanone, KI, Cs<sub>2</sub>CO<sub>3</sub>, DMF, rt, 12 h; (h) NH<sub>4</sub>OAc, AcOH, 100 °C, 1 h; (i) Cu<sub>2</sub>O, NH<sub>4</sub>OH, ethylene glycol, 100 °C, 16 h.

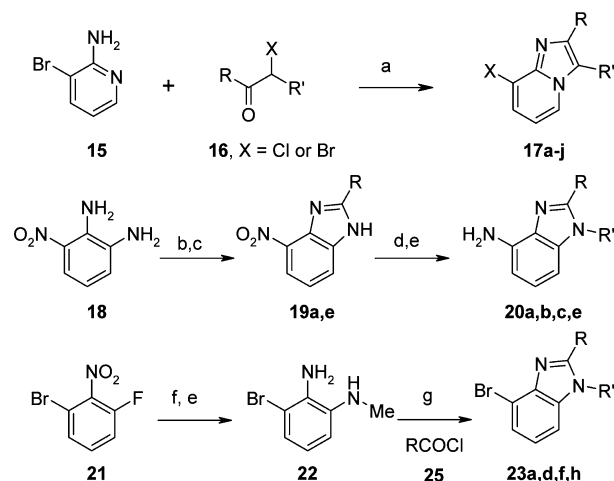
**14** via copper oxide catalyzed amination with ammonium hydroxide.<sup>17</sup>

**Synthesis of Intermediates II. Imidazopyridines.** The imidazopyridine nucleus **17** was prepared by condensation of 2-amino-3-bromopyridine **15** with  $\alpha$ -halo ketones **16** (Scheme 3).

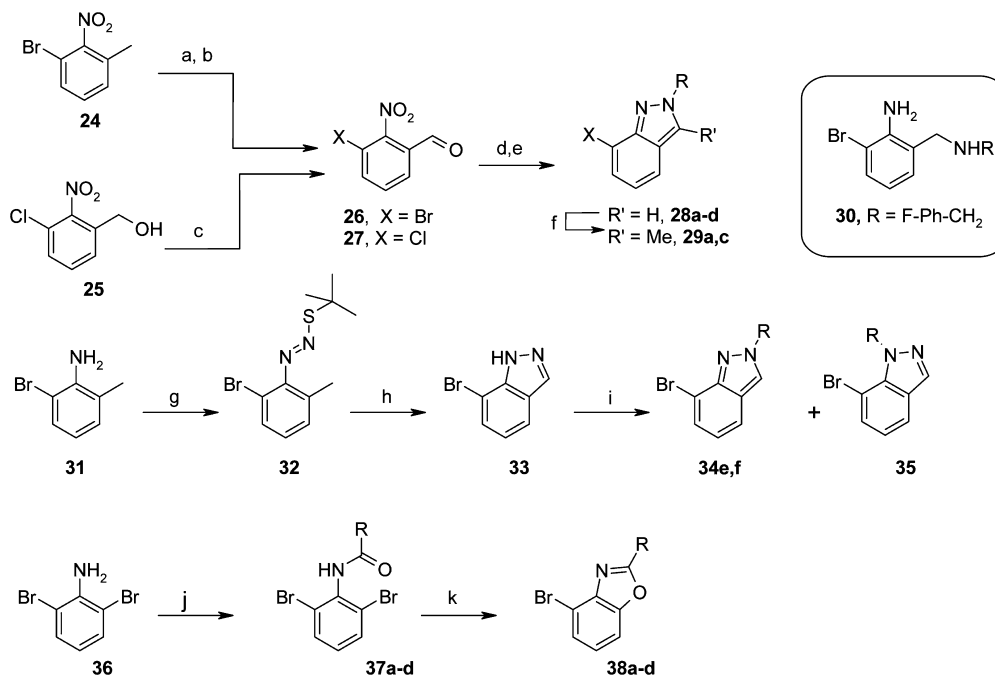
**Benzimidazoles.** The initial synthesis of benzimidazole analogues involved acylation of 1,2-diamino-3-nitrobenzene (**18**) to provide the corresponding anilides (Scheme 3). These compounds were then condensed to a benzimidazole ring system **19** at 150 °C in strong acidic conditions under microwave irradiation. Selective alkylation at N1 of **19** with the corresponding alkyl bromides, followed by reduction of the nitro moiety, gave the desired 1,2-substituted 4-amino-benzimidazoles **20**(a,b,c,e).

Alternatively, benzimidazoles **23**(a,d,f,h) were prepared from 2-bromo-6-fluoro-nitrobenzene (**21**). Aromatic nucleophilic substitution on **21** with methylamine followed by reduction of the nitro functionality provided aniline **22**, which was cyclized with acyl derivatives **25** to provide **23** in good yields.

**Indazoles.** Condensation of 3-bromo-2-nitrotoluene **24** with dimethylformamide dimethyl acetal (DMF-DMA) in the presence of pyrrolidine, followed by oxidation with NaIO<sub>4</sub>, gave 3-bromo-2-nitrobenzaldehyde **26** in a modest 20% yield over two steps (Scheme 4). Alternatively, oxidation of the commercially available 3-chloro-2-nitrobenzyl alcohol **25** gave

Scheme 3. Synthesis of Imidazopyridines and Benzimidazole Building Blocks<sup>a</sup>

<sup>a</sup>Reagents and conditions: (a) EtOH, reflux, 4 h; (b) RCOCl, Et<sub>3</sub>N, CH<sub>2</sub>Cl<sub>2</sub>, rt, 2 h; (c) AcOH, HCl, MW 150 °C, 30 min; (d) LiHMDS, R'Br, THF, 0–150 °C, 1–4 h; (e) Fe, AcOH, 60 °C, 1 h; (f) MeNH<sub>2</sub>, EtOH, 0 °C–rt, 15 h; (g) Et<sub>3</sub>N, CH<sub>2</sub>Cl<sub>2</sub>, rt, 15 h then AcOH, HCl, 100 °C, 2 h.

Scheme 4. Synthesis of Indazole and Benzoxazole Building Blocks<sup>a</sup>

<sup>a</sup>Reagents and conditions: (a) DMF–DMA, pyrrolidine, 115 °C, 22 h; (b) NaIO<sub>4</sub>, DMF/H<sub>2</sub>O, 3 h, rt; (c) PCC, CH<sub>2</sub>Cl<sub>2</sub>, rt, 2 h; (d) R(CH<sub>2</sub>)<sub>n</sub>NH<sub>2</sub>, sodium triacetoxyborohydride, HOAc, 1,2-dichloroethane, rt, 3 h; (e) SnCl<sub>2</sub>·2H<sub>2</sub>O, EtOH, 40 °C, 16 h; (f) LDA, THF, –78 to 0 °C, 15 min, MeI, –78 °C to rt, 16 h; (g) (1) NaNO<sub>2</sub>, 6N aq HCl soln, H<sub>2</sub>O, 30 min, 60 °C, (2) *t*-butylmercaptan, EtOH, 1 h, 0 °C; (h) KO<sup>t</sup>Bu, DMSO, 2 h, rt; (i) R<sub>2</sub>SO<sub>4</sub>, toluene, 16 h, 110 °C or RBr, *N*-methyl-dicyclohexylamine, DMF, 16 h, 30 °C; (j) RCOCl, THF, rt, 15 h; (k) CuI, 1,10-phenanthroline, Cs<sub>2</sub>CO<sub>3</sub>, DME, 90 °C, 15 h.

the 3-chloro analogue **27**, which was also used to synthesize the final products. Reductive amination of benzaldehydes **26** and **27** with the corresponding anilines or benzylamines, followed by reduction of the nitro group with concomitant cyclization to the indazole nucleus, provided **28**.<sup>21</sup> The 3-position of **28a** and **28c** was also methylated using lithium diisopropyl amide (LDA) and methyl iodide in THF to provide bromo indazoles **29a** and **29c**, respectively.

This synthetic route proceeded smoothly when the R substituent at the 2-position of indazoles was an aromatic ring. When R was an alkyl substituent, the major product of the cyclization step (e) in Scheme 4 was a reduced diamino-derivative such as **30**, which was not isolated. Therefore an alternative route for the preparation of the 2-alkyl indazoles was applied, starting from 2-bromo-6-methylaniline **31**. Diazotation of **31** followed by condensation with *t*-butylmercaptan afforded diazene **32**. Subsequently, **32** underwent cyclization to indazole **33** by treatment with potassium *t*-butylate.<sup>22</sup> *N*-Alkylation of **33**, either with a dialkylsulfate, or with an alkylhalide, gave a mixture of the two regioisomers **34** and **35**, which could be separated via chromatography.

**Benzoxazoles.** The synthesis of benzoxazole analogues is shown in Scheme 4. Acylation of dibromoaniline **36** with the corresponding acyl chlorides provided anilides **37**. In turn, these compounds were submitted to cyclization via Ullmann-type coupling conditions in the presence of a catalytic Cu(I)–phenanthroline system<sup>23</sup> to give bromobenzoxazoles **38** in good to excellent yields.

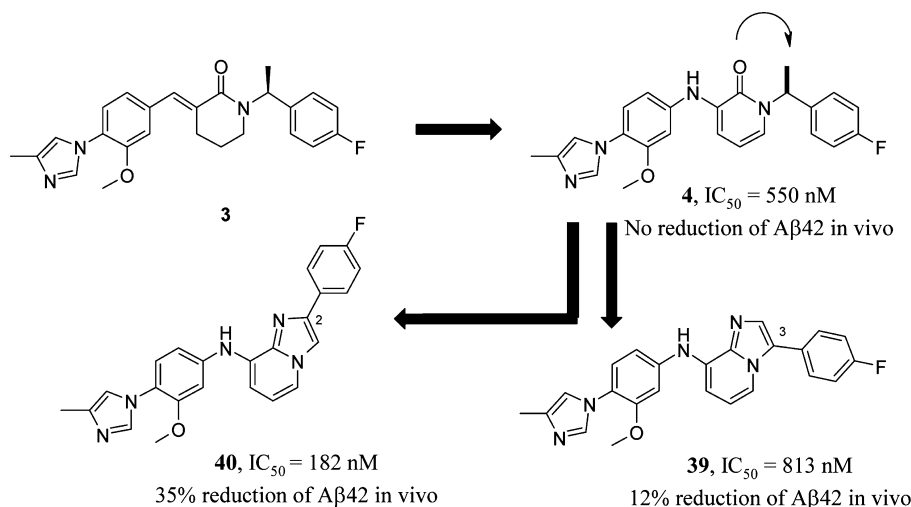
## ■ BIOLOGY

**Cellular In Vitro Assay.** All compounds were tested using SKNBE2 cells carrying the APP 695–wild type according to

modification of the assay as described.<sup>24</sup> The cell/compound mixtures were incubated overnight at 37 °C, 5% CO<sub>2</sub>. Aβ<sub>42</sub> and Aβ<sub>total</sub> concentrations were quantified in the cell supernatant using sandwich immunoassays via the Alphasia technology (Perkin-Elmer). To obtain the reported IC<sub>50</sub> values, the data are calculated as percentage of the maximum amount of Aβ<sub>42</sub> or Aβ<sub>total</sub> measured in the absence of the test compound. The IC<sub>50</sub> represents the concentration of a compound that is required for reducing the Aβ peptide levels by 50%. In this assay, a GSM will lead to a lowering of Aβ<sub>42</sub> while leaving Aβ<sub>total</sub> levels unchanged. Other mechanisms of lowering the Aβ levels, such as γ- or β-secretase inhibition or cytotoxicity, would result in lowering of all Aβ peptides levels, including Aβ<sub>total</sub>. None of the described compounds showed a significant lowering of the Aβ<sub>total</sub> levels up to the highest concentration tested (10 μM), confirming that they are not γ- or β-secretase inhibitors.

**In Vivo Mouse Screening Assay.** To determine the effect on Aβ<sub>42</sub> and Aβ<sub>total</sub> levels upon acute administration of a compound in vivo, nontransgenic CD1 mice were used. Compounds were formulated as suspensions in 20% of Captisol (a sulfobutyl ether of β-cyclodextrin) in water and administered as a single oral dose of 30 mg/kg. After four hours, the animals were sacrificed and their brains dissected in two. One half was used for quantification of Aβ levels using sandwich immunoassays. The other half was analyzed for compound levels and compared to compound levels in blood plasma collected at the same time point. Each quoted value is the mean of at least six animals. Changes in Aβ peptide levels are expressed as a percentage relative to untreated animals. Reduction of Aβ peptide levels of greater than 20% are considered significant. In all runs, compound **3** was dosed as the positive control. In



Scheme 5. Rationale for the Synthesis of Imidazopyridine 40<sup>a</sup>

<sup>a</sup>Mouse in vivo at 30 mpk po after 4 h ( $n = 6$ ) expressed as a percentage of A $\beta$ 42 lowering in brain compared with untreated animals.

agreement with the cellular in vitro data (vide supra), none of the tested compounds showed a significant lowering of the A $\beta$ total levels.

Further biological experiments are explained in the next section and detailed in the Experimental Section or Supporting Information.

## RESULTS AND DISCUSSION

**Imidazopyridines.** To regain the loss in potency, when going from cinnamide 3 to aminopyridone 4 (Figure 1), we set up to investigate conformational restriction of 4. Assuming that the proposed intramolecular hydrogen bond in 4 would indeed mimic the conformation of the cinnamide 3, the *N*-pyridone benzyl substituent was targeted, being the most flexible part of the molecule. A bioisosteric replacement of a pyridone by an imidazopyridine heterocycle has been described as a successful strategy for other targets<sup>25</sup> and would preserve the intramolecular hydrogen bond arrangement present in 4. The 4-fluorophenyl ring present in both 3 and 4 can be oriented in two ways on the imidazopyridine ring, and both regioisomers were prepared (39 and 40, Scheme 5). Only regioisomer 40, in which the aromatic ring was attached to the 2-position, showed an improvement of in vitro activity.<sup>26</sup> Although with an  $IC_{50}$  of 182 nM still lower in potency than cinnamide 3, this now translated in vivo into a 35% reduction of A $\beta$ 42 levels in mouse brain 4 h after an oral dose of 30 mg/kg.

Given this result, the influence of various substituents at the 2-position of the imidazopyridine ring in 40 was evaluated. The most relevant data are presented in Table 1. In general, an aromatic substituent at the 2-position of imidazopyridines brought good in vitro potency, with a range of ring substitutions being allowed. For instance, replacing the *para*-fluorine atom on the aromatic ring in 40a by an electron donating *meta*-methoxy group (40b) slightly increased the potency. A reasonable in vitro activity was also achieved with an unsubstituted phenyl ring (40c). The introduction of a weak basic center, such as a 3-pyridyl ring in 40f, led to a loss of primary activity. When the hydrogen atom at the 3-position of the imidazopyridines was replaced by a bulkier group, such as a methyl group, potency was improved further, see 40c versus 40d. Most of the compounds in Table 1, which were screened

in vivo in mice, displayed a moderate 20–40% lowering of A $\beta$ 42 brain levels, with total levels of A $\beta$  peptides remaining unchanged. No clear correlation could be observed between in vitro potency and in vivo activity, even upon consideration of

**Table 1. In Vitro/in Vivo Activities, Brain/Plasma Levels, and Solubility for Imidazopyridines**

compd	R'	R	$IC_{50}$ (nM) A $\beta$ 42 <sup>a</sup>	brain levels ( $\mu$ M) <sup>b</sup>	plasma levels ( $\mu$ M) <sup>b</sup>	inhib A $\beta$ 42 vivo (%) <sup>c</sup>
40a	H	4-F-Ph	182	11.7 $\pm$ 0.7	17.2 $\pm$ 0.7	35
40b	H	3-MeO-Ph	138	3.0 $\pm$ 0.3	11.1 $\pm$ 0.7	20
40c	H	Ph	339	16.2 $\pm$ 1.1	26.3 $\pm$ 1.6	15
40d	Me	Ph	78	5.4 $\pm$ 0.4	16.0 $\pm$ 2.0	34
40e	Me	2-CF <sub>3</sub> -Ph	26	1.2 $\pm$ 0.3	4.9 $\pm$ 0.8	44
40f	H	3-pyridyl	1216	nd	nd	nd
40g	H	4-F-Ph-CH <sub>2</sub>	100	6.2 $\pm$ 0.3	17.5 $\pm$ 0.7	44
40h	H	Me	442	13.6 $\pm$ 1.5	15.5 $\pm$ 1.6	33
40i <sup>d</sup>	H	<i>n</i> -Bu	194	4.9 $\pm$ 0.3	10 $\pm$ 0.2	13
40j	H	THP	213	5.6 $\pm$ 0.4	11.3 $\pm$ 0.7	7

<sup>a</sup> $IC_{50}$  represents the concentration of a compound that is required for reducing the A $\beta$ 42 level by 50%. The  $IC_{50}$  values are a mean of at least three determinations. The confidence intervals for the  $IC_{50}$  values are reported in the Supporting Information. <sup>b</sup>Plasma and brain samples were analyzed for the tested compound using a qualified research LC-MS/MS method. Data are expressed as the geometric mean values of at least 4 runs  $\pm$  the standard error of the mean (SEM). nd: not determined. <sup>c</sup>Mouse in vivo at 30 mpk p.o. after 4 h ( $n = 6$ ) expressed as a percentage of A $\beta$ 42 lowering in brain compared with untreated animals. nd: not determined. <sup>d</sup>Mouse in vivo at 20 mpk p.o. after 4 h ( $n = 4$ ) expressed as a percentage of A $\beta$ 42 lowering in brain compared with vehicle treated animals.

compound brain levels. An effort was made to correlate in vivo activity with the estimated free brain concentration, using the fraction unbound in brain ( $f_{u,brain}$ ).<sup>27</sup> For most in vivo active compounds,  $f_{u,brain}$  was less than 0.1% and therefore could not be accurately determined. Nevertheless, we observed that many compounds demonstrated robust vivo activity while the estimated free brain concentration was substantially lower than the in vitro  $IC_{50}$  for  $A\beta_{42}$  lowering. Notably, **40e** was one of the most potent compounds in vivo with 44% lowering of  $A\beta_{42}$  levels after 4 h, despite relatively low brain levels and  $f_{u,brain} < 0.03\%$ . In terms of ADME parameters, most of the 2-aryl substituted analogues had poor kinetic solubility at pH = 7.4 ( $< 2 \mu M$ ) and were cytochrome P450 (CYP) inhibitors and hERG channel binders (data not shown). Replacement of the 2-aryl group on the imidazopyridine nucleus by various alkyl groups (**40h–40j**) resulted in active compounds and did increase the solubility but overall did not improve the ADME profile. Compound **40g**, bearing a benzyl substituent, was one of the most potent analogues in vivo, lowering the  $A\beta_{42}$  levels with 44% in mice at 30 mg/kg per os (po). Upon oral dosing, most analogues of the imidazopyridine series displayed high compound plasma levels despite their low solubility. On the other hand, the most soluble compound within this series, the tetrahydropyranyl (THP) derivative **40j** (kinetic solubility at pH 7.4 =  $75 \mu M$ ), had no significant effect on  $A\beta_{42}$  levels in vivo despite moderate in vitro activity, good brain levels, and  $f_{u,brain} = 1.9\%$ , highlighting again the disconnect between free brain concentrations and vivo activity.

Having identified activity with the imidazopyridines **40**, alternative bicyclic systems were synthesized which also contained a hydrogen bond acceptor in the same position relative to the NH linker (Figure 2). These examples included

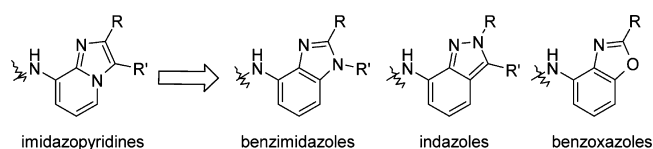


Figure 2. Isosteres of imidazopyridines.

benzimidazole, benzoxazole, and indazole heterocycles. A preference was given to compounds bearing a relatively large substituent R at the 2-position of the heterocyclic nucleus in order to preserve the preferred orientation established within the imidazopyridine series **40**.

**Benzimidazoles.** In general, the benzimidazole series retained the potency of the imidazopyridines and showed a similar SAR profile as for the imidazopyridines (Table 2). The positive influence on potency of an additional substituent R' at the 3-position of the benzimidazole nucleus became even more apparent in this series, with **41a** being at least 10-fold less potent than **41b** and **41c**. For compound **41b**, the high in vitro potency translated into a good in vivo efficacy, this compound lowered the levels of  $A\beta_{42}$  peptides in mouse by 43%. As in the imidazopyridine series, a drop in potency was observed when small aliphatic substituents were introduced at the 2-position of the benzimidazole ring (**41g**). Larger alkyl substituents, such as in **41h**, retained good in vitro potency, and despite a lower metabolic stability (data not shown), this compound displayed high brain levels which translated to a 45% reduction of  $A\beta_{42}$  levels.

Table 2. In Vitro/in Vivo Activities, Brain/Plasma Levels, and Solubility for Benzimidazoles

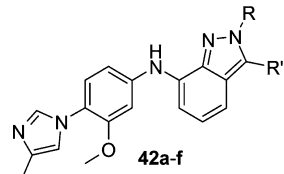
compd	R'	R	$IC_{50}$ $A\beta_{42}$ (nM) <sup>a</sup>	brain levels ( $\mu M$ ) <sup>a</sup>	plasma levels ( $\mu M$ ) <sup>b</sup>	inhib $A\beta_{42}$ vivo (%) <sup>c</sup>
<b>41a</b>	H	4-F-Ph	203	nd	nd	nd
<b>41b</b>	Me	4-F-Ph	17	$7.0 \pm 0.6$	$17.3 \pm 1.3$	43
<b>41c</b>	iPr	4-F-Ph	25	nd	nd	nd
<b>41d</b>	Me	3-OMePh	43	$5.5 \pm 0.5$	$19 \pm 1.0$	45
<b>41e</b>	Me	2,4-F-Ph	69	$10.3 \pm 0.8$	$27 \pm 1.6$	54
<b>41f</b>	Me	4-F-Ph- CH <sub>2</sub>	82	$4.8 \pm 0.4$	$15.7 \pm 1.8$	23
<b>41g</b>	Me	Me	1660	nd	nd	nd
<b>41h</b>	Me	iBu	107	$10.8 \pm 1.3$	$14.1 \pm 1.3$	45

<sup>a</sup> $IC_{50}$  represents the concentration of a compound that is required for reducing the  $A\beta_{42}$  level by 50%. The  $IC_{50}$  values are a mean of at least three determinations. The confidence intervals for the  $IC_{50}$  values are reported in the Supporting Information <sup>b</sup>Plasma and brain samples were analyzed for the tested compound using a qualified research LC-MS/MS method. Data are expressed as the geometric mean values of at least four runs  $\pm$  the standard error of the mean (SEM). nd: not determined. <sup>c</sup>Mouse in vivo at 30 mpk po after 4 h ( $n = 6$ , except for **41(d,f)**, where  $n = 4$ ) expressed as a percentage of  $A\beta_{42}$  lowering in brain compared with untreated animals. nd: not determined.

**Indazoles.** Also compounds from the indazole (Table 3) series turned out to be highly potent. The most active in vitro compounds were substituted on the 2-position of the indazole nucleus with an aromatic ring either directly connected (**42a–c**) or via a methylene spacer (**42d**). Again, additional substitution on the 3-position, for instance with a methyl group, resulted in an improvement of the primary activity (**42c** versus **42b**). In the case of an alkyl substituent on the 2-position, good in vitro activity was retained with a *n*-butyl group (**42f**), whereas a smaller substituent such as a methyl group (**42e**) led to a poorly active compound. Several compounds demonstrated in vivo activity, with up to 41% inhibition of  $A\beta_{42}$  lowering in mouse for compound **42c**.

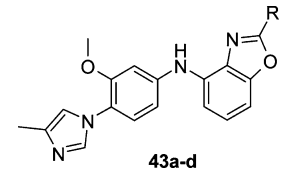
**Benzoxazoles.** Benzoxazole derivatives were clearly less active than their imidazopyridine or benzimidazole analogues (Table 4). For instance 4-F-Ph derivative **43a** was almost 2 orders of magnitude less active than the corresponding imidazopyridine **40a**. In this series, the most active compounds were substituted either with an alkyl substituent on the 2-position of the benzoxazole nucleus (**43d**) or an alkylaryl substituent (**43c**). However, both compounds were not potent enough to significantly reduce  $A\beta_{42}$  levels in vivo.

The high potency of compounds across the imidazopyridine, benzimidazole, and indazole series underlines the benefit of conformational restriction of the original pyridone core in **4**. Additionally, the cyclization promotes a beneficial orientation of the aromatic substituent at the 2-position and allows augmentation of the hydrogen bonding capability of the sp<sup>2</sup> nitrogen at the 1-position. The same heterocyclic nitrogen can form an intramolecular interaction to the NH aniline linker and stabilize an *E*-like conformation similar to **3** and **4**.

**Table 3. In Vitro/in Vivo Activities, Brain/Plasma Levels, and Solubility for Indazoles**


compd	R'	R	IC <sub>50</sub> (nM) Aβ42 <sup>a</sup>	brain levels (μM) <sup>b</sup>	plasma levels (μM) <sup>b</sup>	inhib Aβ42 vivo (%) <sup>c</sup>
42a	Me	2,4-diF-Ph	133	nd	nd	nd
42b	H	3-OMe-Ph	131	6.9 ± 0.3	12.8 ± 0.6	6
42c	Me	3-OMe-Ph	18	4.7 ± 1.0	14.4 ± 0.6	41
42d	H	4-F-Ph-CH <sub>2</sub>	69	6.8 ± 0.6	11.6 ± 1.0	31
42e	H	Me	2252	nd	nd	nd
42f	H	<i>n</i> -Bu	363	nd	nd	nd

<sup>a</sup>IC<sub>50</sub> represents the concentration of a compound that is required for reducing the Aβ42 level by 50%. The IC<sub>50</sub> values are a mean of at least three determinations. The confidence intervals for the IC<sub>50</sub> values are reported in the Supporting Information. <sup>b</sup>Plasma and brain samples were analyzed for the tested compound using a qualified research LC-MS/MS method. Data are expressed as the geometric mean values of at least four runs ± the standard error of the mean (SEM). nd: not determined. <sup>c</sup>Mouse in vivo at 30 mpk po after 4 h (*n* = 6) expressed as a percentage of Aβ42 lowering in brain compared with vehicle treated animals. nd: not determined.

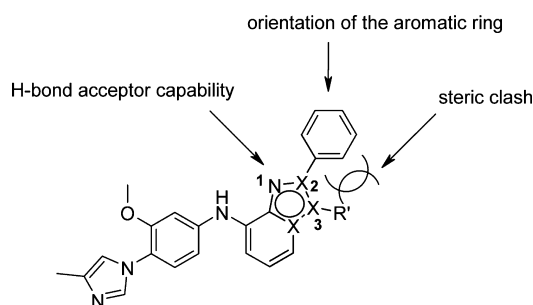
**Table 4. In Vitro/in Vivo Activities, Brain/Plasma Levels, and Solubility for Benzoxazoles**


compd	R	IC <sub>50</sub> (nM) Aβ42 <sup>a</sup>	brain levels (μM) <sup>b</sup>	plasma levels (μM) <sup>b</sup>	inhib Aβ42 vivo (%) <sup>c</sup>
43a	4-F-Ph	5289	11.6 ± 1.1	6.4 ± 0.3	3
43b	2-OMePh	2113	nd	nd	nd
43c	4-F-Ph-CH <sub>2</sub>	696	6.8 ± 0.7	9.4 ± 1.0	15
43d	<i>i</i> Bu	603	10 ± 2.4	4.7 ± 0.9	18

<sup>a</sup>IC<sub>50</sub> represents the concentration of a compound that is required for reducing the Aβ42 level by 50%. The IC<sub>50</sub> values are a mean of at least three determinations. The confidence intervals for the IC<sub>50</sub> values are reported in the Supporting Information. <sup>b</sup>Plasma and brain samples were analyzed for the tested compound using a qualified research LC-MS/MS method. Data are expressed as the geometric mean values of at least four runs ± the standard error of the mean (SEM). <sup>c</sup>Mouse in vivo at 30 mpk po after 4 h (*n* = 6) expressed as a percentage of Aβ42 lowering in brain compared with vehicle treated animals. nd: not determined.

The most potent compounds within the various series are those where the aromatic substituent at the 2-position is pushed out of the plane of the central bicyclic heteroaromatic

ring. This is achieved by the presence of a small alkyl substituent at the 3-position of the imidazopyridines, benzimidazoles, and indazoles (steric clash indicated in Figure 3). The inherent lack of such a substituent in the benzoxazoles

**Figure 3. Factors influencing the potency in the bicyclic heterocycles series.**

can explain the overall lower potency of this series. Non-planarity is also achieved by using ortho-substituted aromatic rings or replacing the aromatic ring with a benzylic or alkyl group. Indeed, in the benzoxazole series all these variations led to an increase in potency (43a versus 43b, 43c, and 43d, respectively).

The carbonyl of the cinnamide 3 and pyridone 4 as well as the heterocyclic sp<sup>2</sup> nitrogen in the series presented here all maintain a hydrogen bond acceptor in the same position. It was expected that this is an important feature for the activity of these molecules. The hydrogen bonding capability of the heterocyclic nitrogen (N1, Figure 3) was evaluated by calculating the minimum electrostatic potential,  $V_{\min}$ , for this atom. This parameter has been shown to be a useful predictor for hydrogen bond strength.<sup>28</sup> A weak correlation ( $r^2$  0.38) was seen between the  $V_{\min}$  descriptor and activity, with more negative values of  $V_{\min}$  and therefore stronger H-bond acceptor capability correlating with potency, see Supporting Information for more details. When comparing analogous molecules, the imidazopyridine and benzimidazoles had the strongest hydrogen bond acceptor potential, while the benzoxazole tended to be the weakest. The hydrogen bond acceptor capabilities of the heterocyclic acceptor were modulated by the introduction of a methyl substituent at the 3-position, as in methyl substituted 41b,  $V_{\min}$  -25.7 kcal/mol, and unsubstituted 41a,  $V_{\min}$  -20.3 kcal/mol. The effects of the methyl are likely 2-fold: electron donating and, as discussed before, disturbing the planarity between the benzimidazole and the 4-F-phenyl- substituent and thereby reducing electron delocalization. Although there was weak overall correlation, a single descriptor is unlikely to capture all properties important for activity and the correlation was seen to break down as more structural diversity at the 2-position was included. Nevertheless, the calculations illustrate an important consideration in the design of the target molecules.

In general, the designed series of compounds showed moderate to excellent in vitro activity, which in some cases translated in very good lowering of Aβ42 peptides in vivo. In contrast to γ-secretase inhibitors, no relevant reduction in Aβtotal levels was observed for any of the tested compounds and no inhibition of Notch processing up to the highest concentration tested (10 μM, data not shown). In all chemical classes, the high potency was accompanied by high lipophilicity (in general, cLogP >5) and a TPSA below 75 Å, explaining the

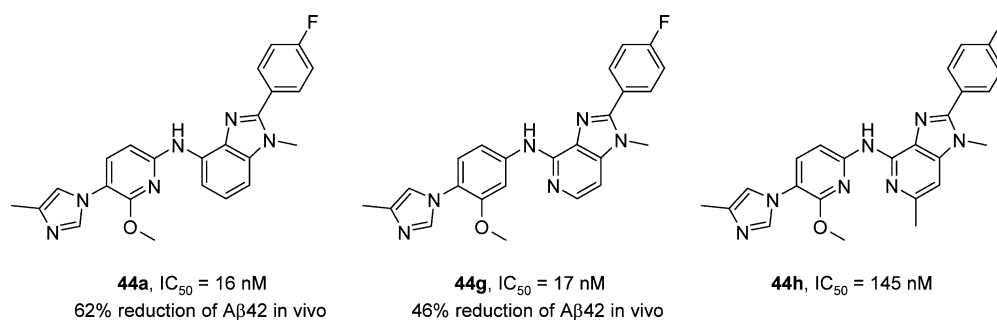


**Figure 4.** Aza benzimidazole analogues. The  $IC_{50}$  values are a mean of at least three determinations.

**Table 5.** In Vitro/in Vivo Activities, Brain/Plasma Levels, Solubility, and hERG Binding of Methoxyphenyl Variations

Cmpd		$IC_{50}$ A $\beta$ 42 (nM) <sup>a</sup>	Brain Levels ( $\mu$ M) <sup>b</sup>	Plasma Levels ( $\mu$ M) <sup>b</sup>	Inhib. A $\beta$ 42 vivo (%) <sup>c</sup>	hERG binding $IC_{50}$ ( $\mu$ M) <sup>d</sup>
<b>44a</b>		16	21.9 $\pm$ 3.2	19.5 $\pm$ 1.1	62	8.5
<b>44b</b>		592	nd	nd	nd	nd
<b>44c</b>		94	6.7 $\pm$ 0.8	22.5 $\pm$ 2.0	36	1.8
<b>44d</b>		183	15.8 $\pm$ 1.1	39.6 $\pm$ 2.7	38	5.2
<b>44e</b>		60	nd	nd	nd	>10
<b>44f</b>		73	12.6 $\pm$ 1.7	30.3 $\pm$ 3.7	29	>10

<sup>a</sup> $IC_{50}$  represents the concentration of a compound that is required for reducing the A $\beta$ 42 level by 50%. The  $IC_{50}$  values are a mean of at least three determinations. The confidence intervals for the  $IC_{50}$  values are reported in the Supporting Information. <sup>b</sup>Plasma and brain samples were analyzed for the tested compound using a qualified research LC-MS/MS method. Data are expressed as the geometric mean values of at least six runs  $\pm$  the standard error of the mean (SEM). nd: not determined. <sup>c</sup>Mouse in vivo at 30 mpk po after 4 h ( $n = 6$ , except for **44a** where  $n = 4$ ) expressed as a percentage of A $\beta$ 42 lowering in brain compared with untreated animals. <sup>d</sup>Inhibition of binding of tritiated dofetilide to the human ether-a-go-go related gene (hERG) expressed in HEK-293 cells.

good brain penetration.<sup>29</sup> However, the majority of compounds also suffered from hERG binding with  $IC_{50}$ s below 1  $\mu$ M, CYP inhibition and low solubility, particularly at pH = 7.4 (data not shown). These unfavorable ADME properties can likely be attributed to the combination of high lipophilicity and low TPSA.<sup>30</sup> Despite the low solubility, most of the compounds had good oral bioavailability, with high levels in plasma and brain. We speculate that this is likely related to the weakly basic character of the imidazole moiety ( $pK_a$  5–6), helping to

solubilize the compounds in the acidic environment of the stomach, for subsequent absorption in the small intestine.<sup>31</sup> Among the most potent in vivo  $\gamma$ -secretase modulators were benzimidazoles **41b** and **41e** (Table 2), which prompted us to further explore the benzimidazole series. To improve the drug-likeness, analogues were designed in which the benzimidazole nucleus (see Figure 4) was kept constant while variations were made on the methoxyphenyl ring as illustrated in compounds **44a–44f**, Table 5.



In the majority of these modifications, the in vitro potency remained below 100 nM, which in vivo translated in the reduction of A $\beta$ 42 levels. Gratifyingly, some of the in vitro ADME parameters were also improved. For example, where compound **41b** inhibited the hERG channel with an IC<sub>50</sub> of 2  $\mu$ M, several of the analogues had an IC<sub>50</sub> above 5  $\mu$ M. Compound **44a** showed the best in vivo lowering of A $\beta$ 42 peptides (62%) in mouse brain 4 h after a dose of 30 mg/kg po, most likely related to the improved brain/plasma ratio compared to **41b** and other **44** analogues. Additional nitrogen analogues **44g** and **44h** were also prepared (Figure 4). Compound **44g**, with the N-atom transferred to the benzimidazole and ortho to the aniline linker, maintained the in vitro activity but showed a lower reduction of the A $\beta$ 42 peptides. Interestingly, with ortho N-atoms present in both adjacent rings to the amino linker as in **44h**, the in vitro activity of **44h** was reduced 10-fold compared to **44a** or **44g**. This may be due to an electronically induced unfavorable torsion angle between the two heteroaromatic rings in **44h**.

Compound **44a** remained the best analogue of the benzimidazole series and also one of the most potent GSMs reported to date. The compound was extensively evaluated for its in vitro ADME properties and in vivo potency in several species. The most relevant physicochemical and in vitro data are tabulated in Table 6. The metabolic stability of **44a** was shown to be good across multiple species with a low turnover in human, mouse, and rat microsomes and a moderate turnover in dog microsomes.<sup>32</sup> In human liver microsomes, no reactive metabolites were observed upon trapping experiments with glutathione or cyanide (data not shown). **44a** was a moderate to weak inhibitor of cytochromes P450, with IC<sub>50</sub> values varying from 2.9 to more than 30  $\mu$ M for the different isoforms in human liver microsomes. No genotoxicity alerts were found in the Ames II<sup>33</sup> or GreenScreen HC<sup>34</sup> tests. In accordance with the high lipophilicity of **44a**, over 98% plasma protein binding was observed across species. The weak affinity of **44a** to bind to the hERG channel (IC<sub>50</sub> 8.5  $\mu$ M) translated into only a weak effect on the potassium membrane current recorded with an automated patch-clamp system (30% inhibition at 3  $\mu$ M versus 17% for vehicle). Compound **44a** was poorly soluble across pH range (<0.001 mg/mL at pH 4 and pH 7.4, Table 6), but it did solubilize in a strongly acidic environment (1.2–2.3 mg/mL in 0.01 N HCl).<sup>31</sup> To have an estimate of the solubility of **44a** in the gastro-intestinal tract (GI tract), the solubility was determined also in the fasted-state and fed-state simulated intestinal fluid buffers (FaSSIF and FeSSIF respectively, Table 6).<sup>35</sup> In the FeSSIF test, **44a** showed an improved, albeit low solubility of 20  $\mu$ g/mL (Table 6). The fact that **44a** had a moderate melting point of 139 °C (see Experimental Section) would also suggest a better solubility across the GI tract than that determined with the pH 4 and pH 7.4 buffers.<sup>36</sup> **44a** displayed a moderate permeability in MDRI-expressing LLC-PK1 cells (LLC-MDR1,  $8 \times 10^{-6}$  cm/s, Table 6),<sup>37</sup> with no indication of P-glycoprotein mediated efflux (0.5 efflux ratio).

In addition, **44a** was screened on 51 receptors and transporters and 37 enzymes in a selectivity screen performed at CEREP.<sup>38</sup> Selectivity overall was good, and the only interactions greater than 50% at 10  $\mu$ M were with NK3 (71%) and with the Na<sup>+</sup> channel (site 2, 60%).

For the in vivo evaluation, **44a** was first tested further in mouse at multiple time points at a dose of 10 and 30 mg/kg po and including measurement of A $\beta$ 38 (Figure 5). A dose

Table 6. In Vitro Drug-Like Profile of **44a**

assay	<b>44a</b>
LogP	5.25
Metabolic Stability (% Conversion) <sup>a</sup>	
human	6
mouse	0
rat	16
dog	37
CYP450 Inhibition, IC <sub>50</sub> ( $\mu$ M) <sup>b</sup>	
3A4 (midazolam)	8.7
3A4 (testosterone)	2.9
2D6 (dextrometorphan)	3.6
2C9 (tolbutamide)	21.9
2C19 (S-mephenytoin)	3.5
1A2 (phenacetin)	>30
Genotoxicity	
Ames II <sup>31</sup>	negative
GreenScreen HC <sup>32</sup>	negative
Plasma Protein Binding (% free)	
human	0.13
mouse	0.04
rat	0.04
dog	0.03
hERG patch clamp (%inh, at 3 $\mu$ M)	30
Thermodynamic Solubility	
buffer pH 4.0	<0.001 mg/mL
buffer pH 7.4	<0.001 mg/mL
0.01N HCl	1.17–2.33 mg/mL
FaSSIF	0.003 mg/mL
FeSSIF	0.020 mg/mL
Permeability (LLC-MDR1 Cells) <sup>c</sup>	
Papp (A–B) (10 <sup>-6</sup> cm/s)	8
Papp (B–A) (10 <sup>-6</sup> cm/s)	4

<sup>a</sup>Metabolism after incubation of **44a** at 1  $\mu$ M with liver microsomes for 15 min.<sup>30</sup> <sup>b</sup>Inhibition of the metabolism of isoform specific substrates (given in parentheses) in human liver microsomes. The IC<sub>50</sub> values are given as a mean of three determinations. <sup>c</sup>A–B = apical to basolateral; B–A = basolateral to apical.

dependent reduction in A $\beta$ 42 was observed, with a concomitant increase in A $\beta$ 38 levels. As expected for a GSM, no significant change in A $\beta$  total level was observed, although at 8 h a tendency of reduction was observed. After 24 h, A $\beta$  levels were normalized, except for the A $\beta$ 42 level at the 30 mg/kg dose, where still some reduction appeared to be present ( $77 \pm 3\%$  versus vehicle). In this experiment, an additional analysis was performed at 48 h, at which time-point also A $\beta$ 42 levels had returned to normal ( $101 \pm 7\%$  versus vehicle, plasma and brain levels of **44a** below quantifiable limit (BQL), data not shown in Figure 5).

Standard pharmacokinetic (PK) studies in multiple species revealed a good and rapid absorption in mouse and dog and a good and slow absorption in rat. Bioavailability for all species was high in rat (95%), mouse (100%), and dog (64%). Detailed PK data can be found in the Supporting Information. Although these PK data were generated with **44a** formulated as a solution

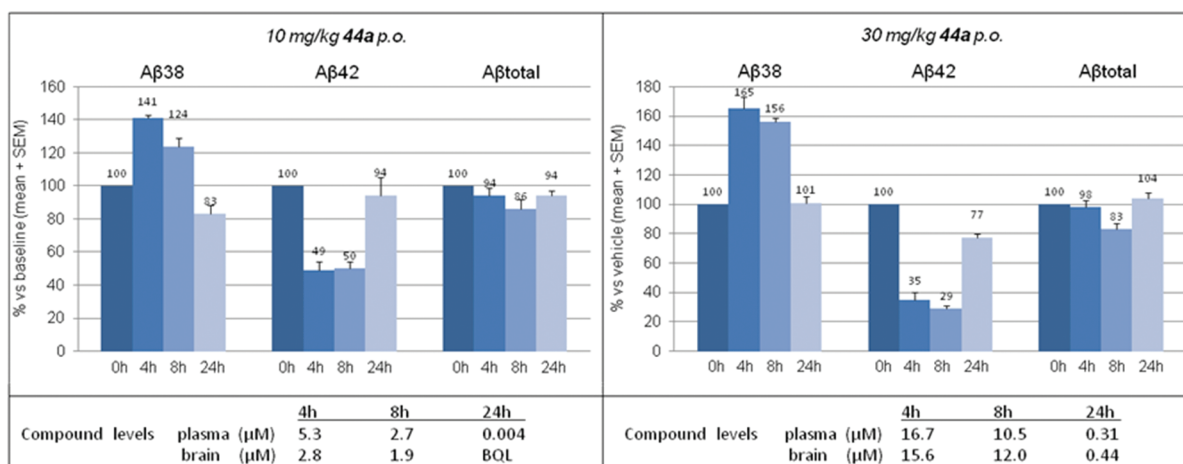


**Figure 5.** Changes in mouse brain  $A\beta$ -levels after a single 10 and 30 mg/kg dose of **44a**. Expressed as mean % change versus  $T = 0$  h,  $n = 4$ .

(1 mg/mL in 20% aqueous SBE- $\beta$ -cyclodextrin solution at pH 4), a comparable exposure was observed when dosed as a methocell suspension. Subsequent in vivo experiments were therefore carried out using methocell suspensions. We recently reported on the use of a canine model to evaluate efficacy and safety of  $\gamma$ -secretase inhibitors (GSIs) and GSMs.<sup>39</sup> In Figure 6,

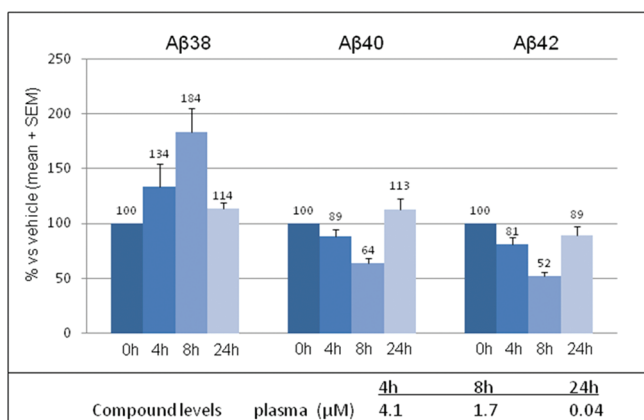


**Figure 6.** Changes in dog CSF  $A\beta$ -levels after a single 20 mg/kg dose of **44a**. Expressed as mean % change versus  $T = 0$  h,  $n = 4$ .

the effect of **44a** on  $A\beta$ 38, 40, and 42 in beagle dog cerebrospinal fluid (CSF) is shown after a single oral dose of 20 mg/kg, as determined via MesoScale Discovery analysis. At 8 h, an increase of 84% in  $A\beta$ 38 and a decrease of 36% and 48% of the longer  $A\beta$ -isoforms  $A\beta$ 40 and  $A\beta$ 42, respectively, were observed. After 24 h, the  $A\beta$  levels were normalized again. Although the compound levels were substantially higher at 4 h than at 8 h, at 4 h only a marginal reduction in  $A\beta$ 40 and  $A\beta$ 42 was seen. This can be explained by a delay in  $A\beta$ -level changes in CSF compared to brain, where the actual production of  $A\beta$  peptides is taking place.

To bridge the data obtained in mouse brain with those in dog CSF, in a subsequent experiment rats were treated with 10 mg/kg of **44a** in order to investigate its efficacy to modulate the release of  $A\beta$ -peptides in brain and CSF within the same species. In addition, the MesoScale analysis was expanded to include the measurement of  $A\beta$ 37 levels. In agreement with the experiments in mouse and dog, a decrease in  $A\beta$ 40 and  $A\beta$ 42 was seen in both brain and CSF. The shorter isoforms  $A\beta$ 37

and  $A\beta$ 38 were increased, with an especially strong increase in  $A\beta$ 37 of 4-fold in brain and 8-fold in CSF (Figure 7). Apart from this difference in change for the shorter  $A\beta$  species, in rat no significant difference or time delay was observed for the  $A\beta$  changes in brain versus CSF.

## CONCLUSIONS

The present studies described the successful application of conformational restriction of aminopyridone **4** into pyridone isosteres such as imidazopyridines, benzimidazoles, benzoxazoles, and indazoles, resulting in new series of GSMs with good in vitro and in vivo activity. The potency was enhanced further by inducing nonplanarity between the central bicyclic heterocycle and the pendant 2-substituent. (Figure 3). Despite the low solubility across the series, good oral bioavailability combined with acceptable brain penetration resulted in considerable reductions in  $A\beta$ 42 levels in mouse brain without significant changes in  $A\beta$ total levels. Replacement of the methoxyphenyl ring with a methoxypyridyl ring has led to **44a** with an improved drug-like profile and enhanced in vivo activity. Benzimidazole analogue **44a** had an  $IC_{50}$  of 16 nM in lowering  $A\beta$ 42 in a cellular assay and displayed good in vivo activity across species such as mouse, rat, and dog. In all three species, a typical  $\gamma$ -secretase modulatory profile was observed with a decrease in the longer  $A\beta$ -isoforms  $A\beta$ 40 and  $A\beta$ 42 and an increase in the shorter isoforms  $A\beta$ 37 and  $A\beta$ 38. Unlike carboxylic acid-derived GSMs recently described<sup>40</sup> with no effect on  $A\beta$ 40 levels, **44a** is efficient in lowering  $A\beta$ 40, suggesting a different mode of interaction with the  $\gamma$ -secretase complex. The especially strong increase in the short  $A\beta$ -peptides  $A\beta$ 37 and  $A\beta$ 38 after treatment with **44a** is noteworthy. Currently, little is known about the toxicity or relevance to plaque formation of these more soluble isoforms  $A\beta$ 37 and  $A\beta$ 38. Studies with compounds such as **44a** may provide further insight in the role of these isoforms.<sup>8</sup> As many of the GSMs described to date, the series detailed in this paper, including **44a**, is suffering from suboptimal physicochemical properties: low solubility, high lipophilicity, and high aromaticity.<sup>30</sup> For **44a**, this has translated into signs of liver toxicity after dosing in dog at 20 mg/kg.<sup>39</sup> Further optimization of the drug-like properties of this series is ongoing. For this work, **44a** will be serving as a benchmark for potency, as well as in studies toward required changes of  $A\beta$ -levels needed for disease modification of Alzheimer's disease.

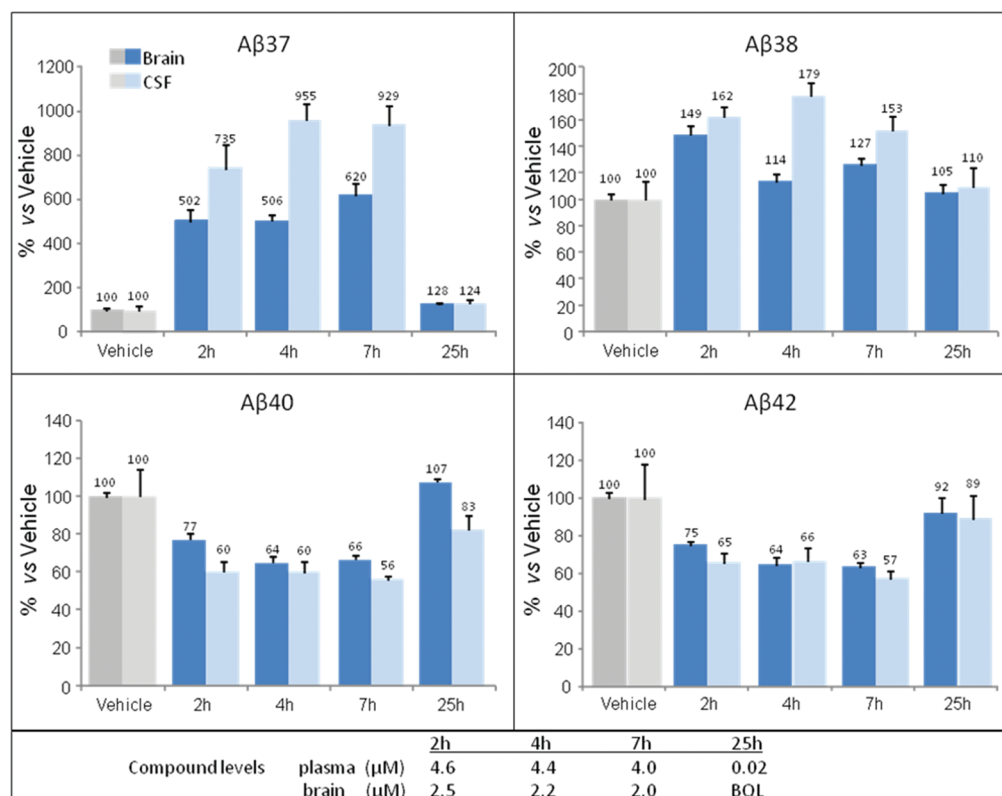


**Figure 7.** Changes in rat brain and CSF A $\beta$  and compound levels of **44a** after a single oral dose (10 mg/kg). Expressed as mean % change versus  $T = 0$  h,  $n = 5$ .

## EXPERIMENTAL SECTION

**Chemistry.** Melting points were determined with a DSC823e (Mettler-Toledo) and were measured with a temperature gradient of 30 °C/min. The reported values are peak values.  $^1\text{H}$  NMR spectra were recorded with Bruker Avance DPX 400 and 360 spectrometers, and chemical shifts ( $\delta$ ) are expressed in parts per million (ppm) with TMS as internal standard. Elemental analyses were performed with a Carlo-Erba EA1110 analyzer. Mass spectral data were obtained via GC-MS analysis, using an Agilent 6890 series GC combined with a 5973N mass selected detector. Combustion analytical results were within 0.4% of the theoretical values except when noted otherwise. For all tested and final compounds where no analytical purity is mentioned, compounds were confirmed >95% pure via HPLC methods. The analytical LC measurement was performed using an Acquity UPLC (Waters) system comprising a binary pump, a sample organizer, a column heater (set at 55 °C), a diode array detector (DAD), and a bridged ethylsiloxane/silica hybrid (BEH) C18 column (1.7  $\mu\text{m}$ , 2.1 mm  $\times$  50 mm; Waters Acquity) with a flow rate of 0.8 mL/min. Two mobile phases (mobile phase A consisting of 0.1% formic acid in  $\text{H}_2\text{O}$ /methanol 95/5; mobile phase B consisting of methanol) were used to run a gradient condition from 95% A and 5% B to 5% A and 95% B in 1.3 min and held for 0.2 min. An injection volume of 0.5  $\mu\text{L}$  was used. Cone voltage was 10 V for positive ionization mode and 20 V for negative ionization mode. Flow from the column was split to a mass spectrometer. The MS detector was configured with an electrospray ionization source. Mass spectra were acquired by scanning from 100 to 1000 in 0.18 s using a dwell time of 0.02 s. The capillary needle voltage was 3.5 kV, and the source temperature was maintained at 140 °C. Nitrogen was used as the nebulizer gas. Sensitive reactions were performed under nitrogen. Commercial solvents were used without any pretreatment. Preparative HPLC purifications were carried out using a Shandon Hyperprep column: C18 base deactivated silica (BDS), 8  $\mu\text{m}$ , 250 g, I.D. 5 cm, and eluting with a gradient of three subsequent mobile phases (phase

A, a 0.25%  $\text{NH}_4\text{HCO}_3$  solution in water; phase B,  $\text{CH}_3\text{OH}$ ; phase C,  $\text{CH}_3\text{CN}$ ).

In general, final compounds obtained as solids were triturated with diisopropylether (DIPE). Alternatively, some compounds were precipitated and isolated as HCl salt by dissolving them in diethylether, followed by the addition of a 1N HCl solution in diethylether.

Compounds **3**<sup>13</sup> and **4**<sup>14a</sup> were synthesized according to literature procedures.

**1-(2-Methoxy-4-nitro-phenyl)-4-methyl-1H-imidazole (7a).** A mixture of 1-chloro-2-methoxy-4-nitrobenzene (150 g, 0.8 mol), 4-methyl-1H-imidazole (131.3 g, 1.6 mol), and  $\text{K}_2\text{CO}_3$  (110.5 g, 0.8 mol) in DMSO (1.5 L) was reacted in an autoclave under a  $\text{N}_2$  atmosphere for 6 h at 150 °C. The reaction mixture was poured into ice-water (6 L). The solid was filtered and washed with water, and then it was dissolved in  $\text{CH}_2\text{Cl}_2$  and further washed with water. The residue was partitioned between  $\text{CH}_2\text{Cl}_2$  and water. The organic layer was dried over  $\text{MgSO}_4$ , filtered, and then the filtrate was concentrated. The residue was purified by chromatography over silica gel (eluent:  $\text{CH}_2\text{Cl}_2$ /methanol 100/0 to 97/3). The desired fractions were collected and the solvent was evaporated. The residue was triturated in DIPE, filtered off and dried to give 48.5 g (26%) of **7a**; mp 136.9 °C.  $^1\text{H}$  NMR (360 MHz,  $\text{DMSO}-d_6$ )  $\delta$  (ppm) 2.17 (s, 3 H), 3.99 (s, 3 H), 7.31 (s, 1 H), 7.70 (d,  $J = 8.4$  Hz, 1 H), 7.95 (dd,  $J = 8.8, 2.5$  Hz, 1 H), 7.97–8.01 (m, 2 H). MS (ESI)  $m/z$  234 [ $\text{M} + \text{H}$ ]<sup>+</sup>.

**3-Methoxy-4-(4-methyl-imidazol-1-yl)-phenylamine (8a).** To a solution of **7a** (48.5 g, 0.21 mol) in MeOH (1 L) was added Pd/C (10%, 5.0 g), and the resulting suspension was stirred at 50 °C under an atmospheric pressure of  $\text{H}_2$  overnight, until 3 equiv of  $\text{H}_2$  were absorbed. The catalyst was filtered over dicalite. The filtrate was concentrated, and the resulting residue was suspended in DIPE and stirred for 1 h. The solid was filtered and dried to yield 39.9 g (94%) of **8a**; mp 128.3 °C.  $^1\text{H}$  NMR (360 MHz,  $\text{DMSO}-d_6$ )  $\delta$  (ppm) 2.10 (s, 3 H), 3.67 (s, 3 H), 5.37 (br s, 2 H), 6.17 (dd,  $J = 8.0, 2.2$  Hz, 1 H), 6.34 (d,  $J = 2.2$  Hz, 1 H), 6.88 (s, 1 H), 6.91 (d,  $J = 8.4$  Hz, 1 H), 7.49 (d,  $J = 1.4$  Hz, 1 H). MS (ESI)  $m/z$  204 [ $\text{M} + \text{H}$ ]<sup>+</sup>.



**4-Methoxy-5-(4-methyl-imidazol-1-yl)-pyridin-2-ylamine (8b).** A solution of *tert*-butyl (5-iodo-4-methoxy-pyridin-2-yl)-carbamate (1.2 g, 3.4 mmol),  $K_2CO_3$  (947 mg, 6.9 mmol), 4-methyl-1*H*-imidazole (394 mg, 4.8 mmol), CuI (653 mg, 3.4 mmol), and 1,10-phenanthroline (618 mg, 3.4 mmol) in DMF (15 mL) was degassed and stirred for 6 days at 120 °C. The reaction mixture was cooled to room temperature and filtered through dicalite. The filtrate was concentrated, and the residue was dissolved in EtOAc and washed with a saturated aqueous  $NaHCO_3$  solution and brine. The organic layer was dried over  $MgSO_4$ , filtered, and concentrated. The crude residue was purified via reversed phase HPLC to provide 120 mg (17%) of **8b**.  $^1H$  NMR (360 MHz,  $CDCl_3$ )  $\delta$  (ppm) 2.28 (s, 3 H), 3.82 (s, 3 H), 4.65 (br s, 2 H), 6.09 (s, 1 H), 6.79 (br s, 1 H), 7.52 (br s, 1 H), 7.89 (br s, 1 H). MS (ESI)  $m/z$  205  $[M + H]^+$ .

**5-Methoxy-6-(4-methyl-imidazol-1-yl)-pyridin-3-ylamine (8c).**  $Na_2CO_3$  (528 mg, 5 mmol) and 4-methyl-1*H*-imidazole (409 mg, 5 mmol) were added to a solution of 2-chloro-3-methoxy-5-nitro-pyridine (940 mg, 5 mmol) in DMF (10 mL). The reaction mixture was stirred at 100 °C for 16 h, and then it was cooled to room temperature and the solvent was evaporated under reduced pressure. The residue was dissolved in EtOAc and was washed with water. The water layer was extracted with EtOAc, and the combined organic layers were dried over  $MgSO_4$ , filtered, and concentrated. The crude residue (**7c**) was added to a suspension of iron powder (835 mg, 15 mmol) in acetic acid (10 mL). The reaction mixture was stirred at 60 °C for 1 h, after which the solvent was evaporated. The residue was dissolved in EtOAc and washed with a saturated aqueous solution of  $NaHCO_3$  and brine. The organic layer was dried over  $MgSO_4$ , filtered, and concentrated to provide 245 mg (21%) of **8c**, which was used as such in the next reaction. MS (ESI)  $m/z$  205  $[M + H]^+$ .

**5-(4-Methyl-imidazol-1-yl)-pyridin-2-ylamine (8d).** CuI (8.26 g, 43.4 mmol) was added to a solution of  $Cs_2CO_3$  (9.4 g, 28.9 mmol), 4-methyl-1*H*-imidazole (5.9 g, 72.3 mmol), and 5-bromo-pyridin-2-ylamine (5 g, 29 mmol) in DMSO (100 mL). The reaction mixture was stirred at 130 °C for 2 days, after which it was cooled to room temperature, triturated in acetonitrile, and filtered. The filtrate was concentrated, and the residue was dissolved in  $CH_2Cl_2$ . The organic layer was washed with water, dried over  $MgSO_4$ , filtered, and concentrated. The residue was purified by flash column chromatography over silica gel (eluent:  $CH_2Cl_2/(7N NH_3$  in MeOH), 100/0 to 96/4) to provide 160 mg of **8d**. The water layer was concentrated until a precipitate started to form. The solid was filtered, yielding an additional 628 mg of **8d** (15% overall yield) as a single regioisomer.  $^1H$  NMR (360 MHz,  $CDCl_3$ )  $\delta$  (ppm) 2.29 (s, 3 H), 4.68 (br s, 2 H), 6.58 (d,  $J = 8.8$  Hz, 1 H), 6.87 (s, 1 H), 7.42 (dd,  $J = 8.8, 2.56$  Hz, 1 H), 7.60 (s, 1 H), 8.11 (d,  $J = 2.9$  Hz, 1 H). MS (ESI)  $m/z$  175  $[M + H]^+$ .

**6-(4-Methyl-imidazol-1-yl)-pyridin-3-ylamine (8e).** *Step 1. Synthesis of 5-Bromo-2-(4-methyl-imidazol-1-yl)-pyridine.*  $K_2CO_3$  (8.8 g, 63 mmol) and 4-methyl-1*H*-imidazole (3.5 g, 42 mmol) were added to a solution of 2,5-dibromo-pyridine (5 g, 21 mmol) in *N*-methyl-2-pyrrolidone (50 mL). The reaction mixture was stirred at 85 °C for 16 h, and then it was cooled to room temperature and partitioned between  $CH_2Cl_2$  and water. The two layers were separated, and the organic layer was dried over  $MgSO_4$  and concentrated under reduced pressure (85 °C at 10 mmHg) to provide 3.3 g (62%) of the title compound as a mixture of regioisomers (85/10). MS (ESI)  $m/z$  238  $[M + H]^+$ .

*Step 2. Synthesis of 8e.* A 250 mL stainless steel autoclave was charged with a solution of the intermediate from step 1 (2.8 g, 12 mmol) in THF (10 mL). Ammonia (90 mL) and  $Cu_2O$  (90 mg, 0.6 mmol) were added. The autoclave was closed, and the reaction mixture was stirred and heated at 150 °C for 18 h. The mixture was allowed to cool to room temperature and extracted three times with  $CH_2Cl_2$ . The combined organic layers were dried over  $MgSO_4$ , filtered, and concentrated. The residue was purified via reversed phase HPLC to provide 250 mg (12%) of **8e**.  $^1H$  NMR (360 MHz,  $CDCl_3$ )  $\delta$  (ppm) 2.29 (d,  $J = 1.1$  Hz, 3 H), 3.76 (br s, 2 H), 7.11 (d,  $J = 1.1$  Hz, 1 H), 7.11 (s, 1 H), 7.22–7.24 (m, 1 H), 7.93 (dd,  $J = 2.2, 1.5$  Hz, 1 H), 8.07 (d,  $J = 1.5$  Hz, 1 H). MS  $m/z$  175  $[M + H]^+$ .

**3-Fluoro-4-(4-methyl-imidazol-1-yl)-phenylamine (8f).** *Step 1. Synthesis of 1-(2-Fluoro-4-nitro-phenyl)-4-methyl-1H-imidazole (7f).*  $K_2CO_3$  (15.3 g, 111 mmol) and 4-methyl-1*H*-imidazole (9.1 g, 111 mmol) were added to a solution of 3,4-difluoro-nitrobenzene (15 g, 92 mmol) in DMF (200 mL). The reaction mixture was stirred at 125 °C for 4 h. The reaction mixture was cooled down to room temperature, diluted with water, and extracted with EtOAc. The organic layer was dried over  $MgSO_4$  and concentrated. The residue was purified via reversed phase. The desired fractions were collected, and the solvent was evaporated and coevaporated with methanol, yielding 13 g (64%) of **7f**.  $^1H$  NMR (360 MHz,  $CDCl_3$ )  $\delta$  (ppm) 2.32 (s, 3 H), 7.01–7.17 (m, 1 H), 7.51–7.66 (m, 1 H), 7.88 (s, 1 H), 8.08–8.28 (m, 2 H). MS (ESI)  $m/z$  222  $[M + H]^+$ .

*Step 2. Synthesis of 8f.* Intermediate **7f** (7.5 g, 34 mmol) and 1 mL of 4% thiophene solution in DIPE were added to a solution of 1 g of palladium on carbon (10% Pd) in methanol (150 mL). The reaction mixture was stirred at 25 °C under hydrogen atmosphere until 3 equiv of  $H_2$  were absorbed. The catalyst was removed by filtration over dicalite. The filtrate was concentrated, and the residue was triturated in heptane, filtered, and dried in vacuo to 6.4 g (100% yield) of **7f**, which was used as such in the next step. MS (ESI)  $m/z$  192  $[M + H]^+$ .

**1-(4-Bromo-2-methoxy-phenyl)-4-methyl-1H-imidazole (11).** A solution of **8a** (20.0 g, 98.4 mmol) in AcOH (200 mL) was added at 10 °C to a stirred solution of  $NaNO_2$  (7.47 g, 108 mmol) in concd  $H_2SO_4$  (160 mL) at such a rate that the temperature of the reaction was maintained below 10 °C. After addition was completed, the resulting mixture was stirred at room temperature for 30 min before being added dropwise to a stirred solution of CuBr (28.2 g, 197 mmol) in 48% HBr (200 mL). The ensuing reaction was stirred for 1 h and then diluted with ice–water (1 L). The resulting white precipitate was filtered, washed with water, and then suspended in a biphasic mixture of  $CH_2Cl_2$  and saturated aqueous  $Na_2CO_3$  solution (1:1). The resulting slurry was filtered over dicalite. The layers were separated, and the organic layer was washed with a diluted ammonia solution. The organic phase was dried over  $MgSO_4$ , filtered, and concentrated to give a first batch of **11** (8.1 g) as a brown solid. The aqueous filtrate was brought to pH = 10 by addition of solid  $Na_2CO_3$  and then extracted 3 times with  $CH_2Cl_2$ . The combined organic extracts were washed with diluted ammonia until the disappearance of the blue color of the water phase. The organic phase was dried over  $MgSO_4$  and filtered. The first batch of **11** was added to the filtrate, which was concentrated to give 24.0 g of the title compound (91.3%) as a brown solid; mp 69.4–70.7 °C.  $^1H$  NMR (360 MHz,  $CDCl_3$ )  $\delta$  (ppm) 2.27 (s, 3 H), 3.83 (s, 3 H), 6.84–6.89 (m, 1 H), 7.10 (dd,  $J = 7.3, 1.1$  Hz, 1 H), 7.13 (d,  $J = 1.8$  Hz, 1 H), 7.15 (s, 1 H), 7.63 (d,  $J = 1.4$  Hz, 1 H). MS (ESI)  $m/z$  267  $[M + H]^+$ .

**6-Bromo-2-methoxy-pyridin-3-ylamine (12).**  $NaOCH_3$  (176 g, 3.3 mol) was added portionwise to a solution of 3-amino-2,6-dibromopyridine (100 g, 0.4 mol) in 1,4-dioxane (1 L), and the resulting mixture was refluxed for 3 h. The reaction mixture was then allowed to cool to room temperature, after which it was poured into an aqueous saturated  $NH_4Cl$  solution (2 L). After stirring for 30 min, diethyl ether (2 L) was added and the bilayer was stirred for 30 min. The layers were separated, and the aqueous layer was diluted with water (1.5 L) and then extracted with diethyl ether (6 × 500 mL). The combined organic layers were washed brine (2 × 500 mL), dried over  $MgSO_4$ , and concentrated. The residue was purified by silica gel chromatography (eluent:  $CH_2Cl_2$ ) to provide 67 g (78%) of **12**, as a brown–orange solid. GC-MS  $m/z$  202.

**6-Bromo-2-methoxy-3-(4-methyl-imidazol-1-yl)-pyridine (13).** *Step 1. Synthesis of N-(6-Bromo-2-methoxy-pyridin-3-yl)-formamide.* A mixture of formic acid (12.8 mL, 340 mmol) and acetic acid anhydride (8.54 mL, 91 mmol) was stirred at room temperature for 40 min. Subsequently, a solution of 3-amino-6-bromo-2-methoxy-pyridine (**12**) (5.0 g, 24.6 mmol) in THF (30 mL) was added dropwise, and the resulting reaction mixture was stirred overnight at 60 °C. The mixture was cooled and poured into ice–water. The resulting solid was filtered, washed with water, and dried to give 5.2 g (76%) of the title compound, which was used as such in the next step. MS (ESI)  $m/z$  231  $[M + H]^+$ .



**Step 2. Synthesis of *N*-(6-Bromo-2-methoxy-pyridin-3-yl)-*N*-(2-oxo-propyl)-formamide.** 1-Chloro-propan-2-one (4.34 g, 46.9 mmol) was added dropwise to a mixture of *N*-(6-bromo-2-methoxy-pyridin-3-yl)-formamide (5.2 g, 18.8 mmol), KI (0.34 g, 2.0 mmol), and Cs<sub>2</sub>CO<sub>3</sub> (21.4 g, 66 mmol) in DMF (50 mL). The reaction mixture was stirred at room temperature overnight, and then it was poured into ice–water and extracted with EtOAc. The combined organic layers were dried over MgSO<sub>4</sub>, filtered, and concentrated. The residue was triturated with DIPE, filtered, and dried to give 4.43 g (82%) of the title compound. <sup>1</sup>H NMR (360 MHz, CDCl<sub>3</sub>) δ (ppm) 2.18 (s, 3 H), 4.00 (s, 3 H), 4.48 (s, 2 H), 7.14 (d, *J* = 8.0 Hz, 1 H), 7.49 (d, *J* = 8.0 Hz, 1 H), 8.23 (s, 1 H). GC-MS *m/z* 286.

**Step 3. Synthesis of **13**.** *N*-(6-Bromo-2-methoxy-pyridin-3-yl)-*N*-(2-oxo-propyl)-formamide (4.4 g, 15.3 mmol) was added to a mixture of NH<sub>4</sub>OAc (5.41 g, 70.2 mmol) in AcOH (50 mL). The reaction mixture was heated at reflux for 1 h, and then it was cooled to room temperature and poured into ice–water. The mixture was brought to pH 9 via the addition of an aqueous NaOH solution (50% w/v), and then it was extracted with EtOAc. The organic layer was separated, dried over MgSO<sub>4</sub>, filtered, and concentrated to give 3.0 g (73%) of **13** as a solid, which was used as such in the next step. <sup>1</sup>H NMR (360 MHz, CDCl<sub>3</sub>) δ (ppm) 2.29 (s, 3 H), 4.03 (s, 3 H), 6.92 (t, *J* = 1.1 Hz, 1 H), 7.17 (d, *J* = 8.0 Hz, 1 H), 7.40 (d, *J* = 7.7 Hz, 1 H), 7.73 (d, *J* = 1.4 Hz, 1 H). MS (ESI) *m/z* 268 [M + H]<sup>+</sup>.

**6-Methoxy-5-(4-methyl-imidazol-1-yl)-pyridin-2-ylamine (**14**).** Cu<sub>2</sub>O (166 mg, 1.16 mmol) and ammonia (24 mL) were added to a solution of **13** (3.12 g, 11.64 mmol) in ethylene glycol (25 mL). The mixture was stirred at 100 °C during 16 h. It was then cooled, diluted with water, and extracted with EtOAc. The organic layer was dried over Na<sub>2</sub>SO<sub>4</sub> and concentrated. The residue was triturated with DIPE to yield 1.51 g (63%) of **14** as a light-brown solid. <sup>1</sup>H NMR (360 MHz, CDCl<sub>3</sub>) δ (ppm) 2.28 (s, 3 H), 3.89 (s, 3 H), 4.45 (br s, 2 H), 6.10 (d, *J* = 8.0 Hz, 1 H), 6.80 (s, 1 H), 7.29 (d, *J* = 8.0 Hz, 1 H), 7.55 (s, 1 H). MS (ESI) *m/z* 205 [M + H]<sup>+</sup>.

**8-Bromo-2-(4-fluoro-phenyl)-imidazo[1,2-*a*]pyridine (**17a**).** A solution of 2-amino-3-bromopyridine (50.0 g, 0.29 mol) and 4-fluorophenacyl bromide (75.3 g, 0.35 mol) in ethanol (300 mL) was stirred at reflux temperature for 17 h. After this time, the reaction mixture was cooled to room temperature. The resulting precipitate was filtered, and the filtrate was partially concentrated to result in a second crop of precipitate. The combined precipitates were triturated with acetonitrile and ethanol. The resulting solid was suspended in a saturated aqueous solution of NaHCO<sub>3</sub> (500 mL) and stirred for 30 min. Then, the mixture was extracted with CH<sub>2</sub>Cl<sub>2</sub>. The organic layer was separated, dried over Na<sub>2</sub>SO<sub>4</sub>, and concentrated. The residue was recrystallized from EtOAc, to provide 46.5 g (55%) of **17a** as a white solid; mp 165.3 °C. <sup>1</sup>H NMR (360 MHz, DMSO-*d*<sub>6</sub>) δ (ppm) 6.83 (t, *J* = 6.9 Hz, 1 H), 7.29 (m, 2 H), 7.60 (d, *J* = 7.3 Hz, 1 H), 8.02 (m, *J* = 5.8 Hz, 2 H), 8.53 (s, 1 H), 8.56 (d, *J* = 7.0 Hz, 1 H). MS (ESI) *m/z* 291 [M + H]<sup>+</sup>.

**2-(4-Fluoro-phenyl)-4-nitro-1*H*-benzimidazole (**19a**, R = 4-F-Ph, R' = H).** **Step 1 Synthesis of *N*-(2-amino-3-nitro-phenyl)-4-fluoro-benzamide.** A solution of 1,2-diamino-3-nitrobenzene (1.53 g, 10 mmol), triethylamine (2.78 mL, 20 mmol), and 4-fluorobenzoyl chloride (1.58 g, 10 mmol) in a mixture of CH<sub>2</sub>Cl<sub>2</sub>/acetonitrile (2/1, 75 mL) was stirred at room temperature for 2 h. After this time, the reaction mixture was diluted with CH<sub>2</sub>Cl<sub>2</sub> (20 mL) and washed with water (20 mL). The two layers were separated, and the organic layer was dried over MgSO<sub>4</sub>, filtered, and concentrated. The resulting residue was triturated with DIPE to give 2.3 g (83%) of the title compound; mp 181.5 °C. <sup>1</sup>H NMR (360 MHz, DMSO-*d*<sub>6</sub>) δ (ppm) 6.70 (dd, *J* = 8.6, 7.5 Hz, 1 H), 7.21 (s, 2 H), 7.32–7.42 (m, 2 H), 7.48 (dd, *J* = 7.3, 1.1 Hz, 1 H), 7.99 (dd, *J* = 8.8, 1.4 Hz, 1 H), 8.05–8.16 (m, 2 H), 9.89 (s, 1 H). MS (ESI) *m/z* 551 [2M + H]<sup>+</sup>.

**Step 2. Synthesis of **19a**.** A solution of *N*-(2-amino-3-nitro-phenyl)-4-fluoro-benzamide (1.35 g, 5.0 mmol) and concd aq HCl (0.5 mL, 6.0 mmol) in acetic acid (15.0 mL) was submitted to microwave irradiation at 150 °C, for 30 min. The reaction mixture was cooled to room temperature, and the product precipitated upon cooling. The precipitate was filtered, washed with acetic acid and

DIPE, and then dried to provide 1.00 g (69%) of **19a** as HCl salt. <sup>1</sup>H NMR (360 MHz, DMSO-*d*<sub>6</sub>) δ (ppm) 6.82 (br. s, 2 H), 7.36–7.58 (m, 3 H), 8.16 (t, *J* = 8.0 Hz, 2 H), 8.37–8.56 (m, 2 H). MS (ESI) *m/z* 258 [M + H]<sup>+</sup>.

**2-(4-Fluoro-phenyl)-1-methyl-1*H*-benzimidazol-4-ylamine (**20b**, R = 4-F-Ph, R' = Me).** **Step 1. Synthesis of 2-(4-Fluoro-phenyl)-1-methyl-4-nitro-1*H*-benzimidazole.** A solution of lithium hexamethyldisilazide (1 M in THF, 2.96 mL, 2.96 mmol) was added dropwise at 0 °C to a solution of **19** (290 mg, 0.99 mmol) in THF (10 mL) under a flow of nitrogen, and the resulting mixture was stirred at this temperature for 30 min. Then CH<sub>3</sub>I (92 μL, 1.48 mmol) was added and the resulting mixture was stirred at 55 °C for 12 h. The reaction was quenched with brine. The organic layer was separated, dried over MgSO<sub>4</sub>, filtered, and concentrated. The resulting residue was triturated with a DIPE/2-propanol mixture. The precipitate was filtered and dried to provide 160 mg (60%) of the title compound. <sup>1</sup>H NMR (400 MHz, DMSO-*d*<sub>6</sub>) δ (ppm) 3.97 (s, 3 H), 7.41–7.55 (m, 3 H), 7.93–8.02 (m, 2 H), 8.12 (ddd, *J* = 12.9, 8.1, 0.8 Hz, 2 H). MS (ESI) *m/z* 272 [M + H]<sup>+</sup>.

**Step 2. Synthesis of **20b**.** Iron (812 mg, 14.5 mmol) was added to a solution of 2-(4-fluoro-phenyl)-1-methyl-4-nitro-1*H*-benzimidazole (750 mg, 2.76 mmol) in AcOH (50 mL), and the resulting mixture was mechanically stirred at 60 °C for 1 h. After this time, the solvent was removed under reduced pressure. The resulting residue was dissolved in CH<sub>2</sub>Cl<sub>2</sub> and washed with a saturated aqueous solution of NaHCO<sub>3</sub> and then brine. The organic layer was separated, active charcoal and MgSO<sub>4</sub> were added, and the resulting mixture stirred at room temperature for 20 min. Filtration over dicalite, followed by concentration of the filtrate, yielded 250 mg (37%) of **20b**. <sup>1</sup>H NMR (360 MHz, DMSO-*d*<sub>6</sub>) δ (ppm) 3.77 (s, 3 H), 6.41 (d, *J* = 7.3 Hz, 1 H), 6.73 (d, *J* = 8.0 Hz, 1 H), 6.98 (t, *J* = 7.9 Hz, 1 H), 7.37–7.43 (m, 2 H), 7.84–7.90 (m, 2 H). MS (ESI) *m/z* 242 [M + H]<sup>+</sup>.

**3-Bromo-*N*1-methyl-benzene-1,2-diamine (**22**).** A solution of methylamine in ethanol (8M, 100 mL, 0.8 mol) was added at 0–5 °C to 1-bromo-3-fluoro-2-nitro-benzene (19.8 g, 90 mmol). The mixture was stirred overnight at room temperature, and then the solvent was evaporated and the residue was partitioned between water and CH<sub>2</sub>Cl<sub>2</sub>. The organic layer was dried over MgSO<sub>4</sub>, filtered, and concentrated to provide 20 g (96%) of crude (3-bromo-2-nitro-phenyl)-methyl-amine, which was dissolved in HOAc (150 mL). Iron powder (15 g, 269 mmol) was added, and the resulting suspension was stirred and heated at 60 °C for 1 h. The reaction mixture was concentrated in vacuo, and the residue was partitioned between CH<sub>2</sub>Cl<sub>2</sub> and a saturated aqueous NaHCO<sub>3</sub> solution. The organic layer was dried over MgSO<sub>4</sub>, filtered, and concentrated to give 14 g (80%) of **22**, which was used as such in the next step. <sup>1</sup>H NMR (360 MHz, CDCl<sub>3</sub>) δ (ppm) 2.87 (s, 3 H), 3.73 (br s, 3 H), 6.60 (dd, *J* = 7.8, 1.3 Hz, 1 H), 6.71 (t, *J* = 8.1 Hz, 1 H), 6.95 (dd, *J* = 8.1, 1.1 Hz, 1 H). GC-MS *m/z* 200.

**4-Bromo-2-(4-fluoro-phenyl)-1-methyl-1*H*-benzimidazole (**23a**, R = 4-F-Ph, R' = Me).** 4-Fluoro-benzoylchloride (5.5 g, 34.7 mmol) was added at room temperature to a solution of **22** (10.0 g, 39.8 mmol) and triethylamine (8.05 g, 79.6 mmol) in CH<sub>2</sub>Cl<sub>2</sub> (250 mL), and the resulting mixture was stirred for 15 h. The reaction mixture was quenched with water, and the two layers were separated. The organic layer was dried over MgSO<sub>4</sub>, filtered, and concentrated. The residue was dissolved in HOAc (100 mL), and concd aq HCl (3 mL), and the resulting solution was stirred for 2 h at 100 °C. The solvent was removed by evaporation, and the residue was dissolved in CH<sub>2</sub>Cl<sub>2</sub> and washed with a saturated aqueous NaHCO<sub>3</sub> solution. The organic layer was dried over MgSO<sub>4</sub>, filtered, and concentrated. The residue was triturated with DIPE/2-propanol and then filtered to give 6.8 g (64%) of **23a**. <sup>1</sup>H NMR (400 MHz, DMSO-*d*<sub>6</sub>) δ (ppm) 3.88 (s, 3 H), 7.24 (t, *J* = 7.7 Hz, 1 H), 7.40–7.47 (m, 2 H), 7.49 (dd, *J* = 7.7, 0.8 Hz, 1 H), 7.66 (dd, *J* = 8.1, 0.8 Hz, 1 H), 7.90–7.97 (m, 2 H). MS (ESI) *m/z* 305 [M + H]<sup>+</sup>.

**3-Bromo-2-nitro-benzaldehyde (**26**).** A mixture of 3-bromo-2-nitrotoluene (10 g, 46.3 mmol), *N,N*-dimethylformamide dimethyl acetal (16.5 g, 139 mmol), and pyrrolidine (3.3 g, 46.3 mmol) was heated at 115 °C for 22 h. The reaction mixture was cooled to 0 °C,

and a cooled solution of NaIO<sub>4</sub> (29.7 g, 139 mmol) in DMF (75 mL) and water (100 mL) was added dropwise. After the addition, the reaction mixture was allowed to warm to room temperature. The suspension was filtered on dicalite and washed with EtOAc (400 mL). The filtrate was washed with water (2 × 150 mL), and the organic layer was concentrated. The residue was purified by flash chromatography over silica gel (eluent: heptane/CH<sub>2</sub>Cl<sub>2</sub> 1/1 to 0/1). The product fractions were collected, and the solvent was evaporated to give 2.72 g (20%) of **26a**, which was used as such in the next step. <sup>1</sup>H NMR (360 MHz, CDCl<sub>3</sub>) δ ppm 7.59 (t, *J* = 7.9 Hz, 1 H), 7.92–7.96 (m, 2 H), 9.90 (s, 1 H).

**7-Bromo-2-(3-methoxy-phenyl)-2H-indazole (28b, R = 3-CH<sub>3</sub>O-Ph, R' = H).** *Step 1. Synthesis of (3-Bromo-2-nitro-benzyl)-(3-methoxy-phenyl)-amine.* To a solution of 3-bromo-2-nitro-benzaldehyde (5.5 g, 23.9 mmol), 3-methoxy-aniline (2.94 g, 23.9 mmol), and HOAc (7.18 g, 119 mmol) in 1,2-dichloroethane (60 mL) was added sodium triacetoxyborohydride (7.6 g, 35.8 mmol). The reaction mixture was stirred for 3 h at room temperature. The reaction mixture was diluted with CH<sub>2</sub>Cl<sub>2</sub> and washed with an aqueous 10% K<sub>2</sub>CO<sub>3</sub> solution and brine. The organic layer was dried over MgSO<sub>4</sub>, filtered, and concentrated. The residue was purified via reversed phase HPLC. The desired fraction was collected and the solvent was evaporated, yielding 5.68 g (70%) of the title compound. <sup>1</sup>H NMR (360 MHz, CDCl<sub>3</sub>) δ (ppm) 3.75 (s, 3 H), 4.18 (br s, 1 H), 4.38 (s, 2 H), 6.11 (t, *J* = 2.4 Hz, 1 H), 6.19 (ddd, *J* = 8.1, 2.4, 0.9 Hz, 1 H), 6.27–6.36 (m, 1 H), 7.08 (t, *J* = 8.1 Hz, 1 H), 7.31 (t, *J* = 8.1 Hz, 1 H), 7.48–7.64 (m, 2 H). MS (ESI) *m/z* 337 [M + H]<sup>+</sup>.

*Step 2. Synthesis of 28b.* To a solution of (3-bromo-2-nitro-benzyl)-(3-methoxy-phenyl)-amine (5.68 g, 16.8 mmol) in EtOH (100 mL) was added tin chloride dihydrate (7.6 g, 34 mmol). The reaction mixture was stirred at 40–60 °C overnight. The solvent was evaporated, and CH<sub>2</sub>Cl<sub>2</sub> was added together with a small amount of water. The mixture was filtered on dicalite, and the filtrate was washed with water. The water layer was extracted with CH<sub>2</sub>Cl<sub>2</sub>, and the organic layer was dried over MgSO<sub>4</sub> and concentrated. The residue was purified by flash chromatography on silica gel (eluent: heptane/CH<sub>2</sub>Cl<sub>2</sub> 40/60 to 0/100) to yield 3.63 g (71%) of **27b**. <sup>1</sup>H NMR (360 MHz, CDCl<sub>3</sub>) δ (ppm) 3.92 (s, 3 H), 6.92–7.04 (m, 2 H), 7.39–7.50 (m, 2 H), 7.51–7.59 (m, 2 H), 7.67 (d, *J* = 8.4 Hz, 1 H), 8.49 (s, 1 H). MS (ESI) *m/z* 303 [M + H]<sup>+</sup>.

**7-Bromo-2-(3-methoxy-phenyl)-3-methyl-2H-indazole (29c, R = 3-CH<sub>3</sub>O-Ph, R' = Me).** A 2 M LDA-solution in THF (7.4 mL, 14.8 mmol) was added dropwise to a solution of **28b** (3 g, 9.9 mmol) in THF (50 mL) at –78 °C. The reaction mixture was allowed to warm up to 0 °C, stirred at 0 °C for 5 min, and then cooled again to –78 °C. CH<sub>3</sub>I (0.92 mL, 14.8 mmol) was added, and the reaction mixture was allowed to warm up to room temperature. After stirring for 16 h, water was added and the water layer was extracted with diethyl ether. The organic layer was dried over MgSO<sub>4</sub>, filtered, and concentrated. The residue was purified by flash chromatography on silica gel (eluent: heptane/CH<sub>2</sub>Cl<sub>2</sub> 50/50 to 0/100) to yield 2.2 g (70%) of **29c**. <sup>1</sup>H NMR (360 MHz, DMSO-*d*<sub>6</sub>) δ ppm 2.64 (s, 3 H), 3.85 (s, 3 H), 6.98 (dd, *J* = 8.4, 7.3 Hz, 1 H), 7.10–7.19 (m, 1 H), 7.20–7.29 (m, 2 H), 7.48–7.56 (m, 1 H), 7.58 (d, *J* = 7.3 Hz, 1 H), 7.81 (d, *J* = 8.4 Hz, 1 H). MS (ESI) *m/z* 317 [M + H]<sup>+</sup>.

**N-(2,6-Dibromo-phenyl)-3-methyl-butylamide (37d, R = *i*-Bu).** Isovaleryl chloride (2.9 mL, 23.9 mmol) was added at room temperature to a solution of 2,6-dibromoaniline (2.00 g, 7.98 mmol) in THF (30 mL). The reaction mixture was stirred at room temperature overnight, and then it was diluted with EtOAc and the organic phase was washed with a saturated aqueous NaHCO<sub>3</sub> solution, dried over MgSO<sub>4</sub>, filtered, and concentrated. The residue was triturated with heptane, filtered, extensively washed with heptanes, and then dried to yield 2.19 g (82%) of **37d**. <sup>1</sup>H NMR (360 MHz, CDCl<sub>3</sub>) δ (ppm) 1.09 (d, *J* = 6.2 Hz, 6 H), 2.16–2.41 (m, 3 H), 6.97 (br s, 1 H), 7.03 (t, *J* = 8.1 Hz, 1 H), 7.59 (d, *J* = 8.1 Hz, 2 H). MS (ESI) *m/z* 334 [M + H]<sup>+</sup>.

**4-Bromo-2-isobutyl-benzoxazole (38d, R = *i*-Bu).** A mixture of **37d** (0.21 g, 0.63 mmol), CuI (12 mg, 0.063 mmol), Cs<sub>2</sub>CO<sub>3</sub> (0.31 g, 0.94 mmol), and 1,10-phenanthroline (23 mg, 0.125 mmol) in DME (3 mL) was stirred at 90 °C in a sealed tube overnight. The mixture

was partitioned between water and CH<sub>2</sub>Cl<sub>2</sub>. The organic layer was dried over MgSO<sub>4</sub>, filtered, and concentrated. The residue was purified by flash column chromatography over silica gel (eluent: heptane/CH<sub>2</sub>Cl<sub>2</sub> 30/70) to give 110 mg (69%) of **38d**. <sup>1</sup>H NMR (360 MHz, CDCl<sub>3</sub>) δ (ppm) 1.04 (d, *J* = 6.6 Hz, 6 H), 2.23–2.42 (m, 1 H), 2.85 (d, *J* = 7.3 Hz, 2 H), 7.18 (t, *J* = 8.1 Hz, 1 H), 7.44 (d, *J* = 8.1 Hz, 1 H), 7.48 (d, *J* = 8.1 Hz, 1 H). MS (ESI) *m/z* 254 [M + H]<sup>+</sup>.

**[2-(4-Fluoro-phenyl)-imidazo[1,2-*a*]pyridin-8-yl]-[3-methoxy-4-(4-methyl-imidazol-1-yl)-phenyl]-amine (40a).** Sodium *tert*-butoxide (0.77 g, 8 mmol), BINAP (93 mg, 0.15 mmol), Pd(OAc)<sub>2</sub> (22 mg, 0.1 mmol), and **8a** (0.72 g, 3 mmol) were added to a solution of **17a** (0.58 g, 2 mmol) in toluene (15 mL), and the mixture was purged with N<sub>2</sub> for 5 min. The reaction mixture was stirred and heated at 100 °C overnight under a N<sub>2</sub> atmosphere. The reaction mixture was cooled to room temperature, water was added, and the mixture was extracted with CH<sub>2</sub>Cl<sub>2</sub>. The organic layer was dried over MgSO<sub>4</sub>, filtered, and concentrated. The residue was purified via reversed phase HPLC. The desired fraction was collected, and the solvent was evaporated. The residue was crystallized from CH<sub>3</sub>CN/DIPE. The solid was collected and dried to give 0.42 g (51%) of **40a**; mp 209.2 °C. <sup>1</sup>H NMR (360 MHz, DMSO-*d*<sub>6</sub>) δ (ppm) 2.15 (s, 3 H), 3.80 (s, 3 H), 6.80 (t, *J* = 6.9 Hz, 1 H), 6.98–7.08 (m, 3 H), 7.22–7.34 (m, 4 H), 7.68 (d, *J* = 1.4 Hz, 1 H), 8.01–8.10 (m, 3 H), 8.38 (s, 1 H), 8.46 (s, 1 H). MS (ESI) *m/z* 414 [M + H]<sup>+</sup>. HRMS calcd for C<sub>24</sub>H<sub>21</sub>FN<sub>5</sub>O (M + H)<sup>+</sup>, 414.1730, found, 414.1739.

**[2-(4-Fluoro-phenyl)-1-methyl-1H-benzimidazol-4-yl]-[3-methoxy-4-(4-methyl-imidazol-1-yl)-phenyl]-amine (41 b).** Compound **41b** was prepared starting from **11** and **20b** in a manner identical to the preparation of **40a**. The crude residue was purified via column chromatography on silica gel [eluent: CH<sub>2</sub>Cl<sub>2</sub>/(7N NH<sub>3</sub> in MeOH), 100/0 to 97/3] to give **41b** in 63% yield; mp 130.9 °C. <sup>1</sup>H NMR (360 MHz, DMSO-*d*<sub>6</sub>) δ (ppm) 2.14 (s, 3 H), 3.74 (s, 3 H), 3.86 (s, 3 H), 6.93 (dd, *J* = 8.5, 2.2 Hz, 1 H), 7.01 (s, 1 H), 7.12–7.23 (m, 5 H), 7.43 (t, *J* = 8.8 Hz, 2 H), 7.63 (d, *J* = 1.3 Hz, 1 H), 7.92 (dd, *J* = 8.6, 5.5 Hz, 2 H), 8.46 (s, 1 H). MS (ESI) *m/z* 428 [M + H]<sup>+</sup>. Anal. (C<sub>25</sub>H<sub>22</sub>FN<sub>5</sub>O) C, H, N. HRMS calcd for C<sub>25</sub>H<sub>23</sub>FN<sub>5</sub>O (M + H)<sup>+</sup>, 428.1886; found, 428.1882.

**[2-(3-Methoxy-phenyl)-3-methyl-2H-indazol-7-yl]-[3-methoxy-4-(4-methyl-imidazol-1-yl)-phenyl]-amine (42c).** Cs<sub>2</sub>CO<sub>3</sub> (0.47 g, 1.44 mmol), X-Phos (50 mg, 0.105 mmol), Pd<sub>2</sub>(dba)<sub>3</sub> (44 mg, 0.048 mmol), and **8a** (97 mg, 0.48 mmol) were added to a solution of **28c** (152 mg, 0.48 mmol) in *tert*-butanol (10 mL), and the mixture was purged with N<sub>2</sub> for 5 min. The reaction mixture was stirred and heated at 110 °C for 20 h under a N<sub>2</sub> atmosphere. The reaction mixture was cooled to room temperature, and water was added. The mixture was extracted with CH<sub>2</sub>Cl<sub>2</sub>. The organic layer was dried over MgSO<sub>4</sub>, filtered, and concentrated. The residue was purified by column chromatography on silica gel (eluent: CH<sub>2</sub>Cl<sub>2</sub>/MeOH, 100/0 to 95/5) to yield 0.13 g (62%) of **42c**; mp 184.4 °C. <sup>1</sup>H NMR (360 MHz, DMSO-*d*<sub>6</sub>) δ (ppm) 2.14 (s, 3 H), 2.64 (s, 3 H), 3.75 (s, 3 H), 3.84 (s, 3 H), 6.92–7.00 (m, 2 H), 7.01 (s, 1 H), 7.09–7.16 (m, 3 H), 7.19 (d, *J* = 8.5 Hz, 1 H), 7.23–7.31 (m, 3 H), 7.52 (t, *J* = 8.4 Hz, 1 H), 7.63 (d, *J* = 1.1 Hz, 1 H), 8.33 (s, 1 H). MS (ESI) *m/z* 440 [M + H]<sup>+</sup>. HRMS calcd for C<sub>26</sub>H<sub>26</sub>N<sub>5</sub>O<sub>2</sub> (M + H)<sup>+</sup>, 440.2086; found, 440.2083.

**(2-Isobutyl-benzoxazol-4-yl)-[3-methoxy-4-(4-methyl-imidazol-1-yl)-phenyl]-amine (43d).** Compound **43d** was prepared starting from **8a** and **38a** in a manner identical to the preparation of **42c**, yielding 71% of **43d**. <sup>1</sup>H NMR (360 MHz, CDCl<sub>3</sub>) δ (ppm) 1.05 (d, *J* = 6.7 Hz, 6 H), 2.23–2.36 (m, 1 H), 2.30 (s, 3 H), 2.81 (d, *J* = 7.2 Hz, 2 H), 3.81 (s, 3 H), 6.72 (s, 1 H), 6.86–6.91 (m, 3 H), 7.03–7.09 (m, 1 H), 7.16 (d, *J* = 9.1 Hz, 1 H), 7.19–7.24 (m, 2 H), 7.62 (d, *J* = 1.3 Hz, 1 H). MS (ESI) *m/z* 377 [M + H]<sup>+</sup>. HRMS calcd for C<sub>22</sub>H<sub>25</sub>N<sub>4</sub>O<sub>2</sub> (M + H)<sup>+</sup>, 377.1977; found, 377.1970.

**[2-(4-Fluoro-phenyl)-1-methyl-1H-benzimidazol-4-yl]-[6-methoxy-5-(4-methyl-imidazol-1-yl)-pyridin-2-yl]-amine (44a).** To a solution of **23a** (6.0 g, 19.6 mmol) in *tert*-butanol (250 mL) were added aniline **14** (4.0 g, 19.66 mmol), Pd<sub>2</sub>(dba)<sub>3</sub> (1.44 g, 1.57 mmol), X-Phos (2.25 g, 4.72 mmol), and Cs<sub>2</sub>CO<sub>3</sub> (19.23 g, 59.0 mmol) under a N<sub>2</sub> atmosphere. The reaction mixture was heated at 100 °C for 3 h.



The solvent was evaporated. Then water was added and the mixture was extracted twice with  $\text{CH}_2\text{Cl}_2$ . The combined organic layers were dried over  $\text{MgSO}_4$ , filtered, and concentrated. The residue was purified by flash column chromatography [eluent:  $\text{CH}_2\text{Cl}_2$ /(7N  $\text{NH}_3$  in MeOH) 100/0 to 96/4]. The product fractions were collected and concentrated. The residue was triturated with DIPE and dried, yielding 5.34 g (63.4%) of **44a**; mp 139.3 °C.  $^1\text{H}$  NMR (360 MHz,  $\text{CDCl}_3$ )  $\delta$  (ppm) 2.31 (s, 3 H), 3.86 (s, 3 H), 4.08 (s, 3 H), 6.60 (d,  $J$  = 8.4 Hz, 1 H), 6.84–6.91 (m, 1 H), 7.04 (dd,  $J$  = 8.0, 0.7 Hz, 1 H), 7.22–7.27 (m, 1 H), 7.28–7.32 (m, 1 H), 7.34 (d,  $J$  = 1.0 Hz, 1 H), 7.42 (d,  $J$  = 8.0 Hz, 1 H), 7.62–7.66 (d,  $J$  = 1.0 Hz, 1 H), 7.72–7.80 (m, 2 H), 7.93 (s, 1 H), 8.19 (d,  $J$  = 8.0 Hz, 1 H). ESI(MS)  $m/z$  429  $[\text{M} + \text{H}]^+$ . Anal. ( $\text{C}_{24}\text{H}_{21}\text{FN}_6\text{O}$ ) C, H, N. HRMS calcd for  $\text{C}_{24}\text{H}_{21}\text{FN}_6\text{O}$  ( $\text{M} + \text{H}^+$ ), 429.1839; found, 429.1854.

**[2-(4-Fluoro-phenyl)-1-methyl-1H-benzoimidazol-4-yl]-[4-methoxy-5-(4-methyl-imidazol-1-yl)-pyridin-2-yl]-amine (44b)**. Compound **44b** was prepared starting from **8b** and **23a** in a manner identical to the preparation of **42c**. The crude residue was purified by flash column chromatography over silica gel (eluent:  $\text{CH}_2\text{Cl}_2$ /(7N  $\text{NH}_3$  in MeOH), 100/0 to 96/4), yielding 100 mg (40%) of **44b**.  $^1\text{H}$  NMR (360 MHz,  $\text{DMSO}-d_6$ )  $\delta$  (ppm) 2.15 (s, 3 H), 3.83 (s, 3 H), 3.86 (s, 3 H), 7.05 (s, 1 H), 7.13–7.27 (m, 3 H), 7.45 (t,  $J$  = 9.0 Hz, 2 H), 7.67 (s, 1 H), 6.7.95 (dd,  $J$  = 8.8, 5.5 Hz, 2 H), 8.08 (s, 1 H), 8.32 (d,  $J$  = 7.3 Hz, 1 H), 9.05 (s, 1 H). MS (ESI)  $m/z$  429  $[\text{M} + \text{H}]^+$ . HRMS calcd for  $\text{C}_{24}\text{H}_{22}\text{FN}_6\text{O}$  ( $\text{M} + \text{H}^+$ ), 429.1839; found, 429.1840.

**[2-(4-Fluoro-phenyl)-1-methyl-1H-benzoimidazol-4-yl]-[5-methoxy-6-(4-methyl-imidazol-1-yl)-pyridin-3-yl]-amine (44c)**. Sodium *tert*-butoxide (288 mg, 3.0 mmol), BINAP (94 mg, 0.15 mmol),  $\text{Pd}(\text{OAc})_2$  (23 mg, 0.1 mmol), and **23a** (305 mg, 1 mmol) were added to a solution of **8c** (245 mg, 1.2 mmol) in toluene (15 mL), and the mixture was purged with  $\text{N}_2$  for 5 min. The reaction mixture was stirred and heated at 150 °C for 5 h under microwave irradiation, and then it was cooled to room temperature. Water was added, and the mixture was extracted  $\text{CH}_2\text{Cl}_2$ . The organic layer was separated, dried ( $\text{MgSO}_4$ ), filtered, and concentrated. The residue was purified via reversed phase HPLC, to provide 79 mg (18%) of **44c**.  $^1\text{H}$  NMR (360 MHz,  $\text{DMSO}-d_6$ )  $\delta$  (ppm) 2.16 (s, 3 H), 3.84 (s, 3 H), 3.86 (s, 3 H), 7.14–7.27 (m, 3 H), 7.37 (s, 1 H), 7.43 (t,  $J$  = 9.0 Hz, 2 H), 7.53 (d,  $J$  = 2.2 Hz, 1 H), 7.92 (dd,  $J$  = 8.8, 5.5 Hz, 2 H), 8.03 (d,  $J$  = 2.2 Hz, 1 H), 8.04 (br s, 1 H), 8.69 (s, 1 H). MS (ESI)  $m/z$  429  $[\text{M} + \text{H}]^+$ . HRMS calcd for  $\text{C}_{24}\text{H}_{22}\text{FN}_6\text{O}$  ( $\text{M} + \text{H}^+$ ), 429.1839; found, 429.1853.

**[2-(4-Fluoro-phenyl)-1-methyl-1H-benzoimidazol-4-yl]-[5-(4-methyl-imidazol-1-yl)-pyridin-2-yl]-amine (44d)**. Compound **44d** was prepared starting from **8d** and **23a** in a manner identical to the preparation of **42c**. The residue was purified by flash column chromatography over silica gel (eluent:  $\text{CH}_2\text{Cl}_2$ /(7N  $\text{NH}_3$  in MeOH), 100/0 to 98/2) to provide 50 mg (16%) of **44d**.  $^1\text{H}$  NMR (360 MHz,  $\text{CDCl}_3$ )  $\delta$  (ppm) 2.31 (s, 3 H), 3.86 (s, 3 H), 6.93 (s, 1 H), 6.99–7.06 (m, 2 H), 7.26 (t, 2 H), 7.34 (t,  $J$  = 8.2 Hz, 1 H), 7.53 (dd,  $J$  = 8.8, 2.7 Hz, 1 H), 7.66 (s, 1 H), 7.76 (dd,  $J$  = 8.5, 5.3 Hz, 2 H), 7.92 (s, 1 H), 8.24 (d,  $J$  = 8.0 Hz, 1 H), 8.36 (d,  $J$  = 2.7 Hz, 1 H). MS (ESI)  $m/z$  399  $[\text{M} + \text{H}]^+$ . HRMS calcd for  $\text{C}_{23}\text{H}_{20}\text{FN}_6$  ( $\text{M} + \text{H}^+$ ), 399.1733; found, 399.1724.

**[2-(4-Fluoro-phenyl)-1-methyl-1H-benzoimidazol-4-yl]-[6-(4-methyl-imidazol-1-yl)-pyridin-3-yl]-amine (44e)**. Compound **44e** was prepared starting from **8e** and **23a** in a manner identical to the preparation of **42c**. The crude residue was purified by flash column chromatography over silica gel (eluent:  $\text{CH}_2\text{Cl}_2$ /(7N  $\text{NH}_3$  in MeOH), 100/0 to 98/2). The product fractions were collected, yielding 95 mg (23%) of **44e**.  $^1\text{H}$  NMR (360 MHz,  $\text{CDCl}_3$ )  $\delta$  (ppm) 2.31 (d,  $J$  = 0.7 Hz, 3 H), 3.86 (s, 3 H), 6.95–7.04 (m, 2 H), 7.11 (d,  $J$  = 7.3 Hz, 1 H), 7.17–7.32 (m, 5 H), 7.69–7.80 (m, 3 H), 8.16 (d,  $J$  = 1.1 Hz, 1 H), 8.45 (d,  $J$  = 2.6 Hz, 1 H). MS (ESI)  $m/z$  399  $[\text{M} + \text{H}]^+$ . HRMS calcd for  $\text{C}_{23}\text{H}_{20}\text{FN}_6$  ( $\text{M} + \text{H}^+$ ), 399.1733; found, 399.1767.

**[3-Fluoro-4-(4-methyl-imidazol-1-yl)-phenyl]-[2-(4-fluoro-phenyl)-1-methyl-1H-benzoimidazol-4-yl]-amine (44f)**. Compound **44f** was prepared starting from **8f** and **23a** in a manner identical to the preparation of **42c**. The crude residue was purified by flash column chromatography over silica gel (eluent:  $\text{CH}_2\text{Cl}_2$ /(7N

$\text{NH}_3$  in MeOH), 100/0 to 98/2). The resulting residue was purified further via reversed phase HPLC to provide 95 mg (23%); mp 116 °C.  $^1\text{H}$  NMR (400 MHz,  $\text{CDCl}_3$ )  $\delta$  (ppm) 2.31 (s, 3 H), 3.85 (s, 3 H), 6.92 (s, 1 H), 6.99–7.03 (m, 1 H), 7.06 (dd,  $J$  = 8.7, 2.5 Hz, 1 H), 7.15 (s, 1 H), 7.18–7.30 (m, 6 H), 7.65 (s, 1 H), 7.74 (dd,  $J$  = 8.5, 5.3 Hz, 2 H). MS (ESI)  $m/z$  416  $[\text{M} + \text{H}]^+$ . HRMS calcd for  $\text{C}_{24}\text{H}_{20}\text{F}_2\text{N}_5$  ( $\text{M} + \text{H}^+$ ), 416.1687; found, 416.1680.

**Biology. Cell-Based in Vitro Assay Method.** Screening was carried out using SKNBE2 human neuroblastoma cells carrying the hAPP 69S–wild type, grown in Dulbecco's Modified Eagle's Medium/Nutrient mixture F-12 (DMEM/NUT-mix F-12) (HAM) provided by Invitrogen (cat. no. 10371–029) containing 5% Serum/Fe supplemented with 1% nonessential amino acids, L-glutamine 2 mM, Hepes 15 mM, penicillin 50 U/mL (units/ml), and streptomycin 50  $\mu\text{g}/\text{mL}$ . Cells were grown to near confluency.

The screening was performed using a modification of the assay as described.<sup>24</sup> Briefly, cells were plated in a 384-well plate at  $10^4$  cells/well in Ultraculture (Lonza, BE12–72SF) supplemented with 1% glutamine (Invitrogen, 25030–024), 1% nonessential amino acid (NEAA), penicillin 50 U/mL, and streptomycin 50  $\mu\text{g}/\text{mL}$  in the presence of test compound at different test concentrations. The cell/compound mixture was incubated overnight at 37 °C, 5%  $\text{CO}_2$ . The next day, the media were assayed for  $A\beta_{42}$  and  $A\beta_{\text{total}}$  by two sandwich immunoassays, using the AlphaLisa technology (Perkin-Elmer) according to the manufacturer's instructions. To quantify the amount of  $A\beta_{42}$  in the cell supernatant, monoclonal antibody specific to the C-terminus of  $A\beta_{42}$  (JRF/cA $\beta_{42}$ /26) was coupled to the receptor beads and biotinylated antibody specific to the N-terminus of  $A\beta$  (JRF/A $\beta$ N/25) was used to react with the donor beads. To quantify the amount of  $A\beta_{\text{total}}$  in the cell supernatant, monoclonal antibody specific to the N-terminus of  $A\beta$  (JRF/A $\beta$ N/25) was coupled to the receptor beads and biotinylated antibody specific to the mid region of  $A\beta$  (biotinylated 4G8) was used to react with the donor beads.

**Mouse in Vivo Assay Method.** Compounds were formulated in 20% of Captisol (a sulfobutyl ether of  $\beta$ -cyclodextrin) in water. The compounds were administered as a single oral dose to overnight fasted, male CD1 Swiss Specific Pathogen Free (SPF) mice (Charles River, Germany). After the desired time of treatment (4 h in the screening model), the animals were sacrificed and  $A\beta$  levels were analyzed. Blood was collected by decapitation and exsanguinations in EDTA-treated collection tubes. Blood was centrifuged at 1900g for 10 min (min) at 4 °C and the plasma recovered and flash frozen for later analysis. The brain was removed from the cranium and hindbrain. The cerebellum was removed, and the left and right hemisphere were separated. The left hemisphere was stored at –18 °C for quantitative analysis of test compound levels. The right hemisphere was rinsed with phosphate-buffered saline (PBS) buffer and immediately frozen on dry ice and stored at –80 °C until homogenization for biochemical assays.

Mouse brains were resuspended in 8 volumes of 0.4% diethylamine (DEA)/50 mM NaCl containing protease inhibitors (Roche-11873580001 or 04693159001) per gram of tissue, e.g., for 0.158 g brain, add 1.264 mL of 0.4% DEA. All samples were homogenized in the FastPrep-24 system (MP Biomedicals) using lysing matrix D (MPBio no. 6913–100) at 6 m/s for 20 s. Homogenates were centrifuged at 221300g for 50 min. The resulting high speed supernatants were then transferred to fresh Eppendorf tubes. Nine parts of supernatant were neutralized with 1 part 0.5 M Tris-HCl pH 6.8 and used to quantify  $A\beta$ -peptide levels. To quantify the amount of  $A\beta$ -peptides in the soluble fraction of the brain homogenates, Enzyme-linked immunosorbent assays (ELISA) were used. Briefly, the standards (a dilution of synthetic  $A\beta_{42}$ , Bachem, and  $A\beta_{38}$ , ANASPEC) were prepared in a 1.5 mL Eppendorf tube in Ultraculture, with final concentrations ranging from 10000 to 0.3 pg/mL. The samples and standards were coinubated with HRPO-labeled N-terminal antibodies for  $A\beta_{42}$  and  $A\beta_{38}$  detection and with the biotinylated mid-domain antibody 4G8 for  $A\beta_{\text{total}}$  detection. Then 50  $\mu\text{L}$  of conjugate/sample or conjugate/standards mixtures were added to the antibody-coated plate. The capture antibodies selectively recognize the C-terminal end of  $A\beta_{42}$  and  $A\beta_{38}$  and the N-

terminal end for A $\beta$ -total detection. Antibody JRF/cA $\beta$ 42/26 was used for A $\beta$ 42 detection, antibody J&JPRD/A $\beta$ 38/5 for A $\beta$ 38 detection, and antibody JRF/tA $\beta$ /2 for A $\beta$ total detection. The plate was allowed to incubate overnight at 4 °C in order to allow formation of the antibody–amyloid complex. Following this incubation and subsequent wash steps, the ELISA for A $\beta$ 42 and A $\beta$ 38 quantification was finished by addition of Quanta Blu fluorogenic peroxidase substrate according to the manufacturer's instructions (Pierce Corp., Rockford, IL). A reading was performed after 10–15 min (excitation 320 nm/emission 420 nm). For A $\beta$ total detection, a streptavidine-peroxidase conjugate was added, followed 60 min later by an additional wash step and addition of Quanta Blu fluorogenic peroxidase substrate according to the manufacturer's instructions (Pierce Corp., Rockford, IL). A reading was performed after 10–15 min (excitation 320 nm/emission 420 nm).

**Dog and Rat in Vivo Assays.** For details on the in vivo experimental procedures for the dog experiment; see ref 39. The experiments in rat were carried out using male Sprague–Dawley rats of 180–220 g, which were fasted overnight before dosing. **44a** was dosed via gastric intubation of a 5 mg/mL suspension in 0.5% methocellulose. After the indicated time points (2, 4, 7, and 25 h), the rats were anesthetized in isoflurane, and 50  $\mu$ L of CSF was sampled from the cisterna magna and frozen on dry ice. Then the animals were sacrificed by decapitation, and blood and brain were collected. Further analysis of compound levels and A $\beta$  levels were performed in analogy to the mouse in vivo assay. A $\beta$  levels in dog and rat derived samples were measured using MesoScale Discovery technology-based sandwich immune-assays. The antibodies against A $\beta$ 38 and A $\beta$ 42 were the same as described above. For A $\beta$ 40, the JRF/cA $\beta$ 40/28 antibody was used; for A $\beta$ 37, the antibody JRD/A $\beta$ 37/3 was used.

## ■ ASSOCIATED CONTENT

### ■ Supporting Information

Synthesis and analytical data of all intermediates and final compounds not described in the Experimental Section. Details of the PK studies in mouse, rat, and dog for **44a**. Description of molecular modeling. Confidence intervals for the cellular A $\beta$ 42 IC<sub>50</sub> values. This material is available free of charge via the Internet at <http://pubs.acs.org>.

## ■ AUTHOR INFORMATION

### ■ Corresponding Author

\*Phone: +32-14-606830. Fax: +32-14-605344. E-mail: [hgijsen@its.jnj.com](mailto:hgijsen@its.jnj.com).

### ■ Notes

The authors declare no competing financial interest.

## ■ ACKNOWLEDGMENTS

We thank our co-workers at Cellzome, the members of the Janssen R&D Biology, ADME, and Screening Departments, and the members of the purification and analysis team.

## ■ ABBREVIATIONS USED

AD, Alzheimer's disease; A $\beta$ , amyloid- $\beta$  peptide; ADME, absorption, distribution, metabolism and excretion; APP, amyloid precursor protein; BACE1,  $\beta$ -secretase; C99, C-terminal fragment obtained after cleavage of APP by BACE1; Captisol, a sulfolbutyl ether of  $\beta$ -cyclodextrin; CyP, cytochrome P<sub>450</sub>; FaSSIF, fasted state simulated intestinal fluid; FeSSIF, fed state simulated intestinal fluid;  $f_{u,brain}$ , fraction of compound unbound in brain; GI, gastro-intestinal; GSM,  $\gamma$ -secretase modulator; GSI,  $\gamma$ -secretase inhibitor; hERG, potassium channel encoded by the human ether-à-go-go related gene; mpk, milligram of compound per kilogram of animal body

weight; nd, not determined; NSAIDs, nonsteroidal anti-inflammatory drugs; po, per os

## ■ REFERENCES

- (1) (a) Jakob-Roetne, R.; Jacobsen, H. Alzheimer's disease: from pathology to therapeutic approaches. *Angew. Chem., Int. Ed.* **2009**, *48*, 3030–3059. (b) Berchtold, N. C.; Cotman, C. W. Evolution in the conceptualization of dementia and Alzheimer's disease: Greco-Roman period to the 1960s. *Neurobiol. Aging* **1998**, *19*, 173–189. (c) Tiraboschi, P.; Hansen, L. A.; Thal, L. J.; Corey-Bloom, J. The importance of neurotic plaques and tangles to the development and evolution of AD. *Neurology* **2004**, *62*, 1984–1989.
- (2) Small, D. H.; Cappai, R. Alois Alzheimer and Alzheimer's disease: a centennial perspective. *J. Neurochem.* **2006**, *99*, 708–710.
- (3) (a) Lahiri, D. K.; Ghosh, C.; Ge, Y. W. A proximal gene promoter region for the  $\beta$ -amyloid precursor protein provides a link between development, apoptosis and Alzheimer's disease. *Ann. N. Y. Acad. Sci.* **2003**, *1010*, 643–647. (b) Walsh, D. M.; Selkoe, D. J. Deciphering the molecular basis of memory failure in Alzheimer's disease. *Neuron* **2004**, *44*, 181–193. (c) Tolia, A.; De Strooper, B. Review structure and function of  $\gamma$ -secretase. *Semin. Cell Dev. Biol.* **2009**, *20*, 211–218. (d) Takami, M.; Nagashima, Y.; Sano, Y.; Ishihara, S.; Morishima-Kawashima, M.; Funtamoto, S.; Yasuo, I.  $\gamma$ -Secretase: successive tripeptide and tetrapeptide release from the transmembrane domain of  $\beta$ -carboxyl terminal fragment. *J. Neurosci.* **2009**, *29*, 13042–13052.
- (4) (a) Kreft, A. F.; Martone, R.; Porte, A. Recent advances in the identification of  $\gamma$ -secretase inhibitors to clinically test the A $\beta$  oligomer hypothesis of Alzheimer's disease. *J. Med. Chem.* **2009**, *52*, 6169–6188. (b) D'Onofrio, G.; Panza, F.; Frisardi, V.; Solfrizzi, V.; Imbibo, B. P.; Paroni, G.; Cascavilla, L.; Seripa, D.; Pilotto, A. Advances in the identification of  $\gamma$ -secretase inhibitors for the treatment of Alzheimer's disease. *Expert Opin. Drug Discovery* **2012**, *7*, 19–37.
- (5) Mitani, Y.; Yarimizu, J.; Saita, K.; Uchino, H.; Akashiba, H.; Shitaka, Y.; Ni, K.; Matsuoka, N. Differential effects between  $\gamma$ -secretase inhibitors and modulators on cognitive function in amyloid precursor protein-transgenic and nontransgenic mice. *J. Neurosci.* **2012**, *32*, 2037–2050.
- (6) Oehlich, D.; Berthelot, D. J. -C.; Gijzen, H. J. M.  $\gamma$ -Secretase modulators as potential disease modifying anti-Alzheimer's drugs. *J. Med. Chem.* **2011**, *54*, 669–698.
- (7) (a) Hardy, J. A.; Higgins, G. A. Alzheimer's disease: the amyloid cascade hypothesis. *Science* **1992**, *256*, 184–185. (b) Bergmans, B. A.; De Strooper, B.  $\gamma$ -Secretases: from cell biology to therapeutic strategies. *Neurology* **2010**, *9*, 215–225. (c) Panza, F.; Solfrizzi, V.; Frisardi, V.; Capurso, C.; D'Introno, A.; Colacicco, A. M.; Vendemiale, G.; Capurso, A.; Imbibo, B. P. Disease-modifying approach to the treatment of Alzheimer's Disease. *Drugs Aging* **2009**, *26*, 537–555.
- (8) Karran, E.; Mercken, M.; De Strooper, B. The amyloid cascade hypothesis for Alzheimer's disease: an appraisal for the development of therapeutics. *Nature Rev. Drug Discovery* **2011**, *10*, 698–712.
- (9) Chávez-Gutiérrez, L.; Bammens, L.; Benilova, I.; Vanderstee, A.; Benurwar, M.; Borgers, M.; Lismond, S.; Zhou, L.; Van Cleynenbreugel, S.; Esselmann, H.; Wiltfang, J.; Serneels, L.; Karran, E.; Gijzen, H.; Schymkowitz, J.; Rousseau, F.; Broersen, K.; De Strooper, B. The mechanism of  $\gamma$ -secretase dysfunction in familial Alzheimer disease. *EMBO J.* **2012**, *31*, 2261–2274.
- (10) For comprehensive reviews on work on  $\gamma$ -secretase modulators see: ref 6 (a) (b) Pettersson, M.; Kauffman, G. W.; am Ende, C. W.; Patel, N. C.; Stiff, C.; Tran, T. P.; Johnson, D. S. Novel  $\gamma$ -secretase modulators: a review of patents from 2008 to 2010. *Expert Opin. Ther. Pat.* **2011**, *21*, 205–225. (c) Zettl, H.; Weggen, S.; Schneider, P.; Schneider, G. Exploring the chemical space of  $\gamma$ -secretase modulators. *Trends Pharmacol. Sci.* **2010**, *31*, 402–410. (d) Baumann, S.; Hötteke, N.; Narlawar, R.; Schmidt, B.  $\gamma$ -Secretase as a target for AD. In *Medicinal Chemistry of Alzheimer's Disease*; Gil, A. M., Eds.; Transworld Research Network: Trivandrum, India, 2008; pp 193–224; (e) Garofalo, A. W. Patents targeting  $\gamma$ -secretase inhibition and modulation for the treatment of Alzheimer's disease: 2004–2008. *Expert Opin. Ther. Pat.* **2008**, *18*, 693–703. (f) Tomita, T. Secretase inhibitors and



modulators for Alzheimer's disease treatment. *Expert Rev. Neurother.* **2009**, *9*, 661–679. (g) Pissarnitski, D. Advances in  $\gamma$ -secretase modulation. *Curr. Opin. Drug Discovery* **2007**, *10*, 392–402. (h) Peretto, I.; La Porta, E.  $\gamma$ -Secretase modulation and its promise for Alzheimer's disease: a medicinal chemistry perspective. *Curr. Top. Med. Chem.* **2008**, *8*, 38–46.

(11) (a) Abdul-Hay, S. O.; Edirisinghe, P.; Thatcher, G. R. J. Selective modulation of amyloid- $\beta$  peptide degradation by flurbiprofen, fenofibrate, and related compounds regulates A $\beta$  levels. *J. Neurochem.* **2009**, *111*, 683–695. (b) Van Broeck, B.; Chen, J.-M.; Treton, G.; Desmidt, M.; Hopf, C.; Ramsden, N.; Karran, E.; Mercken, M.; Rowley, A. Chronic treatment with a novel  $\gamma$ -secretase modulator, JNJ-40418677, inhibits amyloid plaque formation in a mouse model of Alzheimer's disease. *Br. J. Pharmacol.* **2011**, *163*, 375–389.

(12) (a) Cheng, S.; Comer, D. D.; Mao, L.; Balow, G. P.; Pleyne, D. Aryl compounds and uses in modulating amyloid  $\beta$ . Patent WO 2004110350, 2004; (b) Kounnas, M. Z.; Danks, A. M.; C., Soan, T. C.; Ackerman, E.; Zhang, X.; Ahn, K.; Nguyen, P.; Comer, D.; Mao, L.; Yu, C.; Pleyne, D.; Digregorio, P. J.; Velicelebi, G.; Stauderman, K. A.; Comer, W. T.; Mobley, W. C.; Li, Y.-M.; Sisodia, S. S.; Tanzi, R. E.; Wagner, S. L. Modulation of  $\gamma$ -Secretase Reduces  $\beta$ -Amyloid Deposition in a Transgenic Mouse Model of Alzheimer's Disease. *Neuron* **2010**, *67*, 769–780.

(13) Kimura, T.; Kawano, K.; Doi, E.; Kitazawa, N.; Shin, K.; Miyagawa, T.; Kaneko, T.; Ito, K.; Takaishi, M.; Sasaki, T.; Hagiwara, H. Preparation of cinnamide, 3-benzylidenepiperidin-2-one, phenylpropionamide compounds as amyloid  $\beta$  production inhibitors. Patent WO 2005115990, 2005.

(14) Similar strategies have been used by others: (a) Huang, X.; Aslanian, R.; Zhou, W.; Zhu, X.; Qin, J.; Greenlee, W.; Zhu, Z.; Zhang, L.; Hyde, L.; Chu, I.; Cohen-Williams, M.; Palani, A. The Discovery of Pyridone and Pyridazine Heterocycles as  $\gamma$ -Secretase Modulators. *ACS Med. Chem. Lett.* **2010**, *1*, 184–187. (b) Qin, J.; Dhondi, P.; Huang, X.; Mandal, M.; Zhao, Z.; Pissarnitski, D.; Zhou, W.; Aslanian, R.; Zhu, Z.; Greenlee, W.; Clader, J.; Zhang, L.; Cohen-Williams, M.; Jones, N.; Hyde, L.; Palani, A. Discovery of fused 5,6-bicyclic heterocycles as  $\gamma$ -secretase modulators. *Bioorg. Med. Chem. Lett.* **2011**, *21*, 664–669. (c) Fischer, C.; Shah, S.; Hughes, B. L.; Nikov, G. N.; Crispino, J. L.; Middleton, R. E.; Szewczak, A. A.; Munoz, B.; Shearman, M. S. Quinazolinones as  $\gamma$ -secretase modulators. *Bioorg. Med. Chem. Lett.* **2011**, *21*, 773–776. (d) Qin, J.; Zhou, W.; Huang, X.; Dhondi, P.; Palani, A.; Aslanian, R.; Zhu, Z.; Greenlee, W.; Cohen-Williams, M.; Jones, N.; Hyde, L.; Zhang, L. Discovery of a potent pyrazolopyridine series of  $\gamma$ -secretase modulators. *ACS Med. Chem. Lett.* **2011**, *2*, 471–476. (e) Wan, Z.; Hall, A.; Sang, Y.; Xiang, J.-N.; Yang, E.; Smith, B.; Yang, G.; Yu, H.; Wang, J.; Lau, L. F.; Li, T.; Zhao, W.; Su, X.; Zhang, X.; Zhou, Y.; Jin, Y.; Tong, Z.; Cheng, Z.; Hussain, I.; Elliott, J. D.; Matsuoka, Y. Pyridine-derived  $\gamma$ -secretase modulators. *Bioorg. Med. Chem. Lett.* **2011**, *21*, 4832–4835. (f) Petterson, M.; Johnson, D. S.; Subramanyam, C.; Bales, K. R.; am Ende, C. W.; Fish, B. A.; Green, M. E.; Kauffman, G. W.; Lira, R.; Mullins, P. B.; Navaratnam, T.; Sakya, S. M.; Stiff, C. M.; Tran, T. M.; Vetelino, B. C.; Xie, L.; Zhang, L.; Pustilnik, L. R.; Wood, K. M.; O'Donnell, C. J. Design and synthesis of dihydrobenzofuran amides as orally bioavailable, centrally active  $\gamma$ -secretase modulators. *Bioorg. Med. Chem. Lett.* **2012**, *22*, 2906–2911. (g) Fischer, C.; Zultanski, S. L.; Zhou, H.; Methot, J. L.; Shah, S.; Nuthall, H.; Hughes, B. L.; Smotrov, N.; Hill, A.; Szewczak, A. A.; Moxham, C. M.; Bays, N.; Middleton, R. E.; Munoz, B.; Shearman, M. S. Triazoloamides as potent  $\gamma$ -secretase modulators with reduced hERG liability. *Bioorg. Med. Chem. Lett.* **2012**, *22*, 3140–3146.

(15) Conformational analysis was performed on molecule 4 with the Molecular Operating Environment (MOE) software (*Molecular Operating Environment 2010.10 (MOE)*; Chemical Computing Group Inc.: Montreal Quebec Canada, 2010, <http://www.chemcomp.com>) using the MMFF94x force field and the LowModeMD approach with default settings. Unfavourable conformers with alternative conformations of the methoxyphenyl relative to the pyridone were at least 6.3 kcal/mol higher in energy. This suggested the preferred orientation would be significantly more likely to occur.

(16) (a) Gijssen, H. J. M.; Bischoff, F. P.; Zhuang, W.; Van Brandt, S. F. A.; Surkyn, M.; Zaja, M.; Berthelot, D. J.-C.; De Cleyn, M. A. J.; Macdonald, G. J.; Oehlich, D. Substituted benzoxazole, benzimidazole, oxazolopyridine and imidazopyridine derivatives as  $\gamma$ -secretase modulators and their preparation and use for the treatment of diseases. Patent WO 2010094647, 2010; (b) Gijssen, H. J. M.; Velter, A. I.; Macdonald, G. J.; Bischoff, F. P.; Wu, T.; Van Brandt, S. F. A.; Surkyn, M.; Zaja, M.; Pieters, S. M. A.; Berthelot, D. J.-C.; De Cleyn, M. A. J.; Oehlich, D. Novel substituted bicyclic heterocyclic compounds as gamma secretase modulators and their preparation and use in the treatment of diseases. Patent WO 2010089292, 2010; (c) Gijssen, H. J. M.; Macdonald, G. J.; Bischoff, F. P.; Tresadern, G. J.; Trabanco-Suarez, A. A.; Van Brandt, S. F. A.; Berthelot, D. J.-C. Preparation of substituted bicyclic imidazole derivatives as gamma secretase modulators. Patent WO 2010070008, 2010; (d) Bischoff, F. P.; Berthelot, D. J.-C.; De Cleyn, M. A. J.; Macdonald, G. J.; Oehlich, D.; Surkyn, M.; Trabanco-Suarez, A. A.; Tresadern, G. J.; Van Brandt, S. F. A.; Velter, A. I.; Borghys, H.; Masungi, C.; Mercken, M.; Gijssen, H. J. M. Discovery of JNJ-42601572, a  $\gamma$ -Secretase Modulator with Potent, Central Activity in Mouse and Dog. 242nd ACS National Meeting, Denver, CO, August 28–September 1, 2011, Abstract MEDI-3.

(17) Lang, F.; Zewge, D.; Houppis, I. N.; Volante, R. P. Amination of aryl halides using copper catalysis. *Tetrahedron Lett.* **2001**, *42*, 3251–3254.

(18) Venuti, M. C.; Stephenson, R. A.; Alvarez, R.; Bruno, J. J.; Strosberg, A. M. Inhibitors of cyclic AMP phosphodiesterase. 3. Synthesis and biological evaluation of pyrido and imidazolyl analogues of 1,2,3,5-tetrahydro-2-oxoimidazo[2,1-b]quinazoline. *J. Med. Chem.* **1988**, *31*, 2136–2145.

(19) Parlow, J. J.; South, M. S. Synthesis of 2-pyridones as tissue factor VIIa inhibitors. *Tetrahedron* **2003**, *59*, 7695–7701.

(20) Kimura, T.; Kawano, K.; Doi, E.; Kitazawa, N.; Takaishi, M.; Ito, K.; Kaneko, T.; Sasaki, T.; Sato, N.; Miyagawa, T.; Hagiwara, H. Preparation of morpholine type cinnamides as amyloid- $\beta$  production inhibitors. U.S. Patent US 20070117798, 2007.

(21) Shi, D.-Q.; Dou, G.-L.; Ni, S.-N.; Shi, J.-W.; Li, X.-Y.; Wang, X.-S.; Wu, H.; Ji, S.-J. A novel and efficient synthesis of 2-aryl-2H-indazoles via SnCl<sub>2</sub>-mediated cyclization of 2-nitrobenzylamines. *Synlett* **2007**, 2509–2512.

(22) Dell'Erba, C.; Novi, M.; Petrillo, G.; Tavani, C. A novel approach to 1H-indazoles via arylazidosulfides. *Tetrahedron* **1994**, *50*, 3529–3536.

(23) Evidar, G.; Batey, R. A. Parallel synthesis of a library of benzoxazoles and benzothiazoles using ligand-accelerated copper-catalyzed cyclizations of *ortho*-halobenzanilides. *J. Org. Chem.* **2006**, *71*, 1802–1808.

(24) Citron, M.; Westaway, D.; Xia, W.; Carlson, G.; Diehl, T.; Levesque, G.; Johnson-Wood, K.; Lee, M.; Seubert, P.; Davis, A.; Kholodenko, D.; Motter, R.; Sherrington, R.; Perry, B.; Yao, H.; Strome, R.; Lieberburg, I.; Rommens, J.; Kim, S.; Schenk, D.; Fraser, P.; St.; George Hyslop, P.; Selkoe, D. J. Mutant presenilins of Alzheimer's disease increase production of 42-residue amyloid  $\beta$ -protein in both transfected cells and transgenic mice. *Nature Med.* **1997**, *3*, 67–72.

(25) Tresadern, G.; Cid, J. M.; Macdonald, G. J.; Vega, J. A.; de Lucas, A. I.; Garcia, A.; Matesanz, E.; Linares, M. L.; Oehlich, D.; Lavreysen, H.; Biesmans, I.; Trabanco, A. A. Scaffold hopping from pyridones to imidazo[1,2-a]pyridines. New positive allosteric modulators of metabotropic glutamate 2 receptor. *Bioorg. Med. Chem. Lett.* **2010**, *20*, 175–179.

(26) An overlay of the 3-D structures of compounds 3 and 40 is provided in the Supporting Information.

(27) Read, K. D.; Braggio, S. Assessing brain free fraction in early drug discovery. *Expert Opin. Drug Metab. Toxicol.* **2010**, *6*, 337–344.

(28) Murray, J. S.; Ranganathan, S.; Politzer, P. Correlations between the solvent hydrogen bond acceptor parameter  $\beta$  and the calculated molecular electrostatic potential. *J. Org. Chem.* **1991**, *56*, 3734–3739.

(29) Ghose, A. K.; Torsten, H.; Hudkins, R. L.; Dorsey, B. D.; Mallamo, J. P. Knowledge-based, central nervous system (CNS) lead

selection and lead optimization for CNS drug discovery. *Chem. Neurosci.* **2012**, *3*, 50–68 and the references therein..

(30) For a recent review regarding the correlation between in vitro potency, ADMET, and physicochemical parameters, see Hann, M. M. Molecular obesity, potency and other addictions in drug discovery. *Med. Chem. Commun.* **2011**, *2*, 349–355 and the references therein..

(31) For a review on factors that influence the oral absorption of drugs, see Hurst, S.; Loi, C.-M.; Brodfuehrer, J.; El-Kattan, A. Impact of physiological, physicochemical and biopharmaceutical; factors in absorption and metabolism mechanisms on the drug oral bioavailability of rats and humans. *Expert Opin. Drug. Metab. Toxicol.* **2007**, *3*, 469–489.

(32) For assay conditions, see: Kantharaj, E.; Tuytelaars, A.; Proost, P. E. A.; Ongel, Z.; van Assouw, H. P.; Gilissen, R. A. H. J. Simultaneous measurement of drug metabolic stability and identification of metabolites using ion-trap mass spectrometry. *Rapid Commun. Mass Spectrom.* **2003**, *17*, 2661–2668.

(33) Gee, P.; Sommers, C. H.; Melick, A. S.; Gidrol, X. M.; Todd, M. D.; Burriss, R. B.; Nelson, M. E.; Klemm, R. C.; Zeiger, E. Comparison of responses of base-specific Salmonella tester strains with the traditional strains for identifying mutagens: The results of a validation study. *Mutat. Res.* **1998**, *412*, 115–130.

(34) Hastwell, P. W.; Chai, L.-L.; Roberts, K. J.; Webster, T. W.; Harvey, J. S.; Rees, R. W.; Walmsley, R. M. High-specificity and high-sensitivity genotoxicity assessment in a human cell line: Validation of the GreenScreen HC GADD45a-GFP genotoxicity assay. *Mutat. Res., Genet. Toxicol. Environ. Mutagen.* **2006**, *607*, 160–175.

(35) Dressman, J. B.; Reppas, C. In vitro–in vivo correlations for lipophilic, poorly water soluble drugs. *Eur. J. Pharm. Sci.* **2000**, *S73–S78*.

(36) Yamaoka, Y.; Roberts, R. D.; Stella, V. J. Low melting phenytoin prodrugs as alternative oral delivery modes for phenytoin: a model for other high-melting sparingly water-soluble drugs. *J. Pharmacol. Sci.* **1983**, *72*, 400–405.

(37) Salama, N. N.; Yang, Z.; Bui, T.; Ho, R. J. Y. MDR1 haplotypes significantly minimize intracellular uptake and transcellular P-gp substrate transport in recombinant LLC-PK1 cells. *J. Pharm. Sci.* **2006**, *95*, 2293–2308.

(38) The CEREP selectivity screen was performed on the following receptors and transporters: A1, A2A, A3, alpha 1, alpha 2, beta 1, AT1, BZD, B2, CCK1, CCKA, D1, D2S, ETA, GABA, GAL2, CXCR2 (IL-8B), CCR1, H1, H2, MC4, MT1 (ML1A), M1, M2, M3, NK2, NK3, Y1, Y2, NTS1 (NT1), delta 2 (DOP), kappa (KOP), mu (MOP), NOP (ORL1), 5-HT1A, 5-HT1B, 5-HT2A, 5-HT2B, 5-HT3, 5-HT5a, 5-HT6, 5-HT7, sst, VPAC1 (VIP1), V1a, Ca<sup>2+</sup> channel (L, verapamil site) (phenylalkylamine), KV channel, SKCa channel, Na<sup>+</sup> channel (site 2), Cl<sup>-</sup> channel (GABA-gated) norepinephrine transporter, and dopamine transporter; and on the following enzymes: PLA2, COX1, COX2, 12-lipoxygenase, PDE2A, PDE3A, PDE4D, PDES, PDE6, ACE, ACE-2, BACE-1, ECE-1, elastase, caspase-3, caspase-8, cathepsin D, cathepsin L, HIV-1 protease, neutral endopeptidase, MMP-1, MMP-3, MMP-9, tryptase, TACE, phosphatase 1B (PTP1B), phosphatase CDC25A, phosphatase MKP1, acetylcholinesterase, MAO-A, MAO-B, HDAC3, HDAC4, HDAC6, HDAC11, sirtuin 1, sirtuin 2.

(39) For a comprehensive study of this modulator's behavior in a dog model, see: Borghys, H.; Tuefferd, M.; Van Broeck, B.; Clessens, E.; Dillen, L.; Cools, W.; Vinken, P.; Straetemans, R.; de Ridder, F.; Gijssen, H.; Mercken, M. A canine model to evaluate efficacy and safety of  $\gamma$ -secretase inhibitors and modulators. *J. Alzheimer's Dis.* **2012**, *28*, 809–822.

(40) Peng, H.; Talreja, T.; Xin, Z.; Cuervo, J. H.; Kumaravel, G.; Humora, M. J.; Xu, L.; Rohde, E.; Gan, L.; Jung, M.; Shackett, M. N.; Chollate, S.; Dunah, A. W.; Snodgrass-Belt, P. A.; Arnold, H. M.; Taveras, A. G.; Rhodes, K. J.; Scannevin, R. H. Discovery of BIIB042, a potent, selective, and orally bioavailable  $\gamma$ -secretase modulator. *ACS Med. Chem. Lett.* **2011**, *2*, 786–791.